



REVIEW ARTICLE

Photocatalytic remediation of persistent organic pollutants (POPs): A review



Van-Huy Nguyen^a, Siwaporn Meejoo Smith^b, Kitirote Wantala^c,
Puangrat Kajitvichyanukul^{d,e,*}

^a Institute of Research and Development, Duy Tan University, Da Nang 550000, Viet Nam

^b Center of Sustainable Energy and Green Materials and Department of Chemistry, Faculty of Science, Mahidol University, Salaya, Nakhon Pathom 73170, Thailand

^c Department of Chemical Engineering, Faculty of Engineering, Khon Kaen University, Khon Kaen 40002, Thailand

^d Department of Environmental Engineering, Faculty of Engineering, Chiang Mai University, Chiang Mai 50200, Thailand

^e Center of Excellence in Materials Science and Technology, Chiang Mai University, Chiang Mai 50200, Thailand

Received 29 February 2020; accepted 23 April 2020

Available online 4 May 2020

KEYWORDS

Persistent Organic Pollutants (POPs);
Photocatalysis;
Environmental remediation;
TiO₂;
Fenton;
photo-Fenton

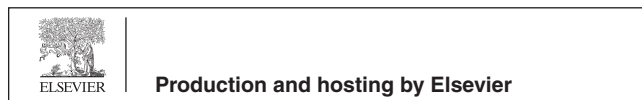
Abstract The release of persistent organic pollutants (POPs) into the environment is an issue of global concern, as the chemicals are stable over a prolonged period resulting in their accumulation in many animals and plants. Although POPs are banned in several countries, many chemicals have been proposed as POP candidates to be added to the existing compounds as defined by the United Nations Stockholm Convention committee. To address the safe disposal and clean-up of such chemicals, new, and especially cost-effective, remediation technologies for POPs are urgently required. This review focuses on existing POPs and the types of remediation processes available for their removal. Particular attention is paid towards photocatalysis using nanocatalysts in this review, due to their effectiveness towards POP degradation, technological feasibility, and energy and cost-efficiency. The underlying principles and the key mechanisms of the photocatalysts based on TiO₂ based materials, metal oxides, light-assisted Fenton systems, framework materials *e.g.* metal-organic frameworks and polyoxometalates, including metal-free and hybrid photocatalysts for POPs cleanup are described for advance applications in solving the POPs contamination in

Abbreviations: CNTs, carbon nanotubes; DDT, 1,1'-(2,2,2-Trichloroethane-1,1-diyl)bis(4-chlorobenzene); HCB, hexachlorobenzene; MOFs, metal-organic frameworks; MOPs, microporous organic polymers; MWCNTs, multi-walled carbon nanotubes; nZVI, nano zero-valent irons; PBDEs, polybrominated diphenyl ethers; PCBs, polychlorinated biphenyl; PCDDs, polychlorinated dibenzodioxins; PCDFs, polychlorinated dibenzofurans; POMs, polyoxometalates; POPs, persistent organic pollutants; rGO, reduced graphene oxide; UV, ultraviolet; ZVI, zero valent irons

* Corresponding author.

E-mail address: puangrat.k@cmu.ac.th (P. Kajitvichyanukul).

Peer review under responsibility of King Saud University.



the environment. The improvements of photocatalytic performance especially the POPs removal mechanism using the conventional and modified process, the design and optimization of photoreactors, and the integration technology are the critical challenges for the emerging pollutants and require intensive research for the forthcoming future.

© 2020 The Authors. Published by Elsevier B.V. on behalf of King Saud University. This is an open access article under the CC BY-NC-ND license (<http://creativecommons.org/licenses/by-nc-nd/4.0/>).

Contents

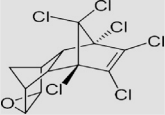
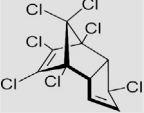
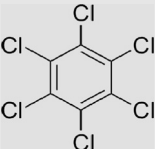
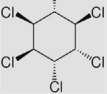
| | |
|---|------|
| 1. Introduction | 8310 |
| 2. Pops background | 8317 |
| 2.1. Categories of POPs | 8317 |
| 2.2. Conventional methods in POP removal. | 8317 |
| 3. Removal of POPs using TiO ₂ photocatalysis | 8320 |
| 3.1. TiO ₂ and its modification photocatalysts. | 8320 |
| 3.1.1. Modification of surface properties and crystal structures | 8320 |
| 3.1.2. Immobilized TiO ₂ on different supports | 8320 |
| 3.1.3. TiO ₂ -doped with the metal/nonmetal nanoparticles | 8322 |
| 3.1.4. Coupling with the semiconductor materials. | 8322 |
| 3.1.5. Hybridizing with the carbonaceous nanomaterials | 8323 |
| 3.1.6. Hybridizing with the addition of oxidants. | 8323 |
| 3.2. Operating conditions, kinetics, and performance in POP removal using TiO ₂ photocatalyst. | 8325 |
| 3.2.1. Effect of POP properties and concentration on the photocatalytic degradation | 8325 |
| 3.2.2. Effect of UV or visible light irradiation | 8326 |
| 3.2.3. Effect of catalyst and catalyst loading | 8326 |
| 3.2.4. Photocatalytic degradation pathway of POPs | 8326 |
| 4. Removal of POPs using Fenton and photo-Fenton reactions. | 8327 |
| 4.1. Removal of POP using Fenton reagent and performance of the system | 8327 |
| 4.2. Removal of POPs using Fenton-like reaction. | 8327 |
| 4.3. Removal of POPs using Photo-Fenton reactions | 8328 |
| 4.4. Removal of POPs using zero valent irons (ZVI) | 8328 |
| 5. Removal of POP using other photocatalysts | 8329 |
| 6. Concluding remarks and perspectives | 8330 |
| Declaration of Competing Interest | 8331 |
| Acknowledgment. | 8331 |
| References. | 8331 |

1. Introduction

Rapid economic growth, energy intensity, industrialization, and urbanization in recent years have created enormous challenges for the environment, human health, and ecosystems (Al-Mulali et al., 2015; Bakirtas and Akpolat, 2018). In particular, the widespread production and utilization, of toxic and hazardous persistent organic pollutants (POPs) have raised significant concerns owing to their environmental impact (Ashraf, 2017; El-Shahawi et al., 2010). A range of POPs, especially organochlorine insecticides, polychlorinated biphenyl (PCBs), polychlorinated dibenzodioxins (PCDDs), polychlorinated dibenzofurans (PCDFs), and polybrominated diphenyl ethers (PBDEs), etc. are mainly from anthropogenic activities and have been widely used in array of products (Jones and de Voogt, 1999; Mato et al., 2001). These POPs, which could reach the environment through agricultural, industrial and municipal activities, have been a threat to ecosystems (Pariatamby and Kee, 2016). It has increased attention to the overuse of pesticides through agricultural activities (Yadav,

2010). Such pesticides have high toxicity, as well as a bioaccumulation potential and are widespread in the environment causing massive contamination. Pesticides have been found everywhere, including soil, water (for example, surface water, groundwater, and drinking water), causing environmental devastation (Katsoyiannis and Samara, 2004; Miranda-García et al., 2011; Pariatamby and Kee, 2016). Currently, many physical, chemical, biological, or combination techniques have been proposed for decomposition and mineralization of POPs. However, conventional POP treatments such as adsorption and coagulation-flocculation, with the sedimentation as the post-treatment, are only solely fixating the toxic compounds without complete removal (Padmanabhan et al., 2006). In another approach, chemical oxidation and biotechnology techniques also face many disadvantages, including high costs with large chemical consumption, incomplete destruction, and prolonged overall treatment time (Dong et al., 2015). Preferential effective techniques for eliminating POPs are those that offer advantages such as highly efficient, ecologically friendly, and technologically reliable techniques that have a relatively

Table 1 Key chemical properties, toxicity and environmental degradation of the well-known POPs.

| Name and Chemical structure | Properties | Sources | Toxicity | Environmental Degradation | References |
|---|---|---|--|---|---|
| Endrin $C_{12}H_8Cl_6O$  | Molecular Weight: 380.9 g/mol Boiling Point: 245 °C Melting Point: 473° F. Solubility: less than 1 mg/mL at 68° F Density:1.7 at 68 °F Vapor Pressure: 2e-07 mm Hg at 77 °F Log Kow: 5.20 Henry's Law constant: 6.4×10^{-6} atm-m ³ /mole | Insecticide, rodenticide and avicide. | Health Effects: Acute toxicity, short-term high- risk effects, reproductive Hazards Exposure Routes: The substance can be absorbed into the body through the skin and by ingestion. The substance can be absorbed into the body by inhalation, through the skin and by ingestion. | Photodegradation half-life is 7 days. Volatilization half-life is 63 days. It is no mobility in soil with half-life 4–8 years. Volatilization from moist soil surfaces is expected to be an important fate process. If released into water, endrin is expected to adsorb to suspended solids and sediment in water. Bioconcentration in aquatic organisms is very high. | (Budavari, 1996; De Bruijn and Hermens, 1991) |
| Heptachlor $C_{10}H_5Cl_7$  | Molecular Weight: 373.3 g/mol Boiling Point: 293°F Melting Point: 203 to 205 °F Solubility: less than 1 mg/mL at 68° F Density:1.66 at 68 °F Vapor Pressure: 0.0003 mm Hg at 77 °F Log Log K _{ow} : 6.10 Henry's Law Constant: 2.94×10^{-4} atm- m ³ /mole | Termite control, seed/seed furrow treatment, and wood treatment. | EPA: Probable human carcinogen. IARC: Possibly carcinogenic to humans. Exposure Routes: Inhalation, skin absorption, ingestion, skin and/or eye contact. | It is stable to daylight, air, moisture, and moderate heat (up to 160 °C). Field dissipation half-lives for heptachlor can range from 40 days to 5.5 yrs. If released into water, heptachlor is expected to adsorb to suspended solids and sediment. | (Budavari, 1996; Hansch and Leo, 1979; Lide, 2000; Simpson et al., 1995; Tomlin, 1994) |
| Hexachlorobenzene C_6Cl_6  | Molecular Weight: 290.7 g/mol Boiling Point: 612 °F at 760 mm Hg Melting Point: 441 to 444 °F Solubility: less than 1 mg/mL at 68° F Water Solubility: 2.18×10^{-8} M Density:2.044 at 75.2 °C Vapor Pressure: 1 mm Hg at 237.9 °F Log K _{ow} : 5.73 Henry's Law Constant: 0.00 atm-m ³ /mole | Pesticide, chemical industry, and automotive industry | Evidence for Carcinogenicity: EPA: Probable human carcinogen. IARC: Possibly carcinogenic to humans. Health Effects: Nervous system, long-term organ toxicity, respiratory system, hematoLogic or reproductive system. | Hexachlorobenzene is not expected to volatilize from dry soil surfaces based upon its vapor pressure. It is persistent to either abiotic or biodegradation processes in soil. If released into water, hexachlorobenzene is expected to adsorb to suspended solids and sediment. The volatilization half-life from a model pond (2 m deep) is estimated as approximately 5 years if adsorption is considered. | (O'Neil, 2006; MacBean, 2008; Hansch et al., 1995; Hartley and Kidd, 1983) |
| α-hexachloro cyclohexane $C_6H_6Cl_6$  | Molecular Weight: 290.83 g/mol Boiling point: 288 °C at 760 mmHg Melting point:159– 160 °C Density (g/cm3): 1.87 at 19 °C | Pesticide, medical uses | Evidence for Carcinogenicity: IARC: Possibly carcinogenic to humans. Health Effects: Nervous system, chronic | Half-life in air is approximately 115 days. It is low mobility in soil and not volatilize from dry soil surfaces. The biodegradation half- life was 90 days in | (Lide, 2000; Schaefer et al., 2015) |

(continued on next page)

Table 1 (continued)

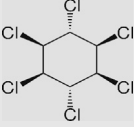
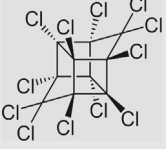
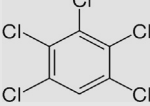
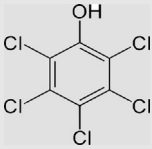


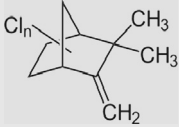
| Name and Chemical structure | Properties | Sources | Toxicity | Environmental Degradation | References |
|---|---|---|---|--|---|
| | Vapor pressure: 4.5×10^{-5} mmHg at 25 °C Solubility: Poor water solubility or insoluble Henry's law constant: 6.86×10^{-6} Log K_{ow} : 3.8 | | (cumulative) toxicity. | moist soil, and 63 days in a soil slurry. | |
| β -hexachloro cyclohexane $C_6H_6Cl_6$ | Molecular Weight: 290.83 g/mol Boiling point: 60 °C at 0.5 mmHg Melting point: 314– 315 °C Density (g/cm ³):1.89 at 19 °C Vapor pressure: 3.6×10^{-7} at 20 °C Solubility: Poor water solubility or insoluble Henry's law constant: 4.5×10^{-7} Log K_{ow} : 3.78 | Pesticide | Evidence for Carcinogenicity: possible human carcinogen. Health effects: Nervous system, chronic (cumulative) toxicity | Half-life in air is estimated to be 28 days. It is low to slight mobility in soil and not volatilize from dry soil surface. It is little to no aerobic biodegradation and slightly anaerobic degradation. If released into water, it is expected to adsorb to suspended solids and sediment. | (Lide, 2000; USEPA, 2020) |
| γ -hexachloro Cyclohexane (or Lindane) $C_6H_6Cl_6$ |  Molecular Weight: 290.83 g/mol Boiling point: 323.4 °C Melting point: 112.5 °C Density (g/cm ³):1.87 at 20 °C Vapor pressure: 3.6×10^{-7} at 20 °C Solubility: Poor water solubility or insoluble Log K_{ow} : 3.72 | Pesticide and Pharmaceutical use | Evidence for Carcinogenicity: possible human carcinogen. Health effects: Skin irritation, burning sensations, itching, dryness, and rash | It is resistant for aerobic degradation in the water and soil. The biodegradation is possible by anaerobic pathway. The biodegradation in soil is depended on its desorption from soil particles. It can bioaccumulate in food chains. | (Lide, 2000; USEPA, 2020) |
| Mirex $C_{10}Cl_{12}$ |  Boiling Point: 485 °C at 1 mm Hg Melting Point: 485 °C Solubility: less than 1 mg/mL at 25 °C Vapor Density: 3×10^{-7} mm Hg at 25 °C Log K_{ow} : 6.89 Henry's Law Constant: 8.11×10^{-4} atm- m ³ /mole | Insecticide, flame-retardant additive in thermoplastic, thermosetting and elastomeric resins, paper, paint rubber, electrical adhesive and textile products. | Evidence for Carcinogenicity: IARC: Possibly carcinogenic to humans. | Mirex is slowly degraded by direct photolysis reaction. It is expected to be immobile in soil and may volatilize from moist soil surfaces. Mirex is very slow to biodegrade in the environment and is expected to have biodegradation half- lives of one year or more in most soils. | (ATSDR, 1995; O'Neil, 2006; |
| Pentachlorobenzene C_6HCl_5 |  Molecular Weight: 250.3 g/mol Boiling Point: 277 °C at 760 mm Hg Melting Point:86.0 °C Solubility:0.831 mg/L at 25 °C Density:1.8342 Vapor Pressure:0.002 mm Hg at | Industrial processes, electrical equipment, solid waste incineration, combustion of coal and combustion of various biomasses | Evidence for Carcinogenicity: not classifiable as to human carcinogenicity. Exposure Routes: The substance can be absorbed into the body by | Half-life in air is estimated to be 277 days. It can be removed from the atmosphere by wet and dry deposition. It is not expected to volatilize from dry soil surfaces. It resistant to | (Hansch et al., 1995; Shiu and Ma, 2000; Bailey, et al., 2009) |

Table 1 (continued)

| Name and Chemical structure | Properties | Sources | Toxicity | Environmental Degradation | References |
|---|--|--|---|---|--|
|  <p>Pentachlorophenol C₆Cl₅OH or C₆HCl₅O</p> | <p>25 °C Log K_{ow}: 5.18 Henry's Law Constant = 7.03e-04 atm-m³/mole</p> <p>Molecular Weight: 266.3 g/mol Boiling Point: 309 to 310 °C at 760 mm Hg (with decomposition) Melting Point: 191 °C Solubility: less than 1 mg/mL at 25 °C Density: 1.978 g/mL Vapor Pressure: 0.00011 mm Hg at 20 °C; 40 mm Hg at 211.22 °C Log K_{ow}: 5.12 Henry's Law Constant: 2.45 × 10⁻⁸ atm-m³/mole</p> | <p>Product of fungus metabolism, wood preservative, surface disinfectant</p> | <p>inhalation and by ingestion.</p> <p>Evidence for Carcinogenicity: EPA: Likely to be carcinogenic to humans. IARC: Carcinogenic to humans Health Effects: Acute toxicity, chronic (cumulative) toxicity, nervous System, disturbances, reproductive hazards</p> | <p>degradation in laboratory soil tests with half-lives of 194 and 345 days reported in duplicate experiments. Pentachlorobenzene is resistant to biodegradation under aerobic conditions.</p> <p>It is possibly degraded in the atmosphere by reaction with photochemically-produced hydroxyl radicals with the estimated half-life 29 days. Half-life in soil is approximately weeks to months It may photodegrade rapidly in surface water when exposed to direct sun light. Half-life in soil is approximately weeks to months.</p> <p>It is not expected to react with photochemically-produced hydroxyl radicals or be susceptible to direct photolysis by sunlight. It is no mobility in soil. It can volatilize from moist soil surfaces If released into water, it is expected to adsorb to suspended solids and sediment.</p> | <p>(O'Neil, 2006; Hansch and Leo, 1979; Ide et al., 1972; Murthy et al., 1979; Rao and Davidson, 1982)</p> |
|  <p>Perfluorooctanesulfonyl fluoride C₈F₁₈O₂S</p> | <p>Molecular Weight: 502.12 g/mol Boiling Point: 154 °C Solubility: In water: 1.41 × 10⁻⁴ mg/L at 25 °C Density: 1.824 g/mL at 25 °C Vapor Pressure: 5.75 mm Hg at 25 °C Log K_{ow}: 7.84</p> | <p>surfactant, in paper and packaging treatment, and surface protectant</p> | <p>Evidence for Carcinogenicity: No data</p> <p>Health Effects: decreased HDL cholesterol</p> | <p>It is not expected to react with photochemically-produced hydroxyl radicals or be susceptible to direct photolysis by sunlight. It is no mobility in soil. It can volatilize from moist soil surfaces If released into water, it is expected to adsorb to suspended solids and sediment.</p> | <p>(Haynes, 2010; Olsen et al., 2004)</p> |
|  <p>Perfluorooctane sulfonic acid C₈HF₁₇O₃S</p> | <p>Molecular Weight: 500.13 g/mol Boiling Point: 249 °C Density: 1.25 at 25 °C Solubility: 3.2 × 10⁻³ mg/L at 25 °C Vapor Pressure: 2.0 × 10⁻³ mm Hg at 25 °C Log K_{ow}: 4.49</p> | <p>surface treatments, paper protection, and performance chemicals</p> | <p>Health effects: Causes severe skin burns and eye damage. May cause respiratory irritation</p> | <p>Half-life in air is estimated to be 115 days. It is not volatilize from dry soil surfaces and it is resistant to biodegradation.</p> | <p>(Savu, 1999; ATSDR, 2015, OECD, 2002)</p> |
|  <p>Toxaphene</p> | <p>Boiling Point: 155 °C Melting Point: 65 to 90 °C Solubility: less than 1 mg/mL at 19 °C Density: 1.65 Vapor Pressure: 0.4 mm Hg at 25 °C</p> | <p>Insecticide</p> | <p>Evidence for Carcinogenicity: EPA: Probable human carcinogen. IARC: Possibly carcinogenic to humans. Health Effects:</p> | <p>Half-lives in aerobic soil for the toxaphene mixture range from 1 to 11 years. It is not readily aerobic biodegradation for toxaphene components with more than 3 chlorine</p> | <p>(Esaac and Matsumura, 1980; Rossberg et al., 2006; Saleh, 1991; USEPA, 1998; U.S. Environmental Protection Agency Report,</p> |

(continued on next page)

Table 1 (continued)

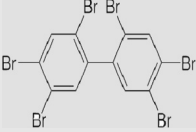
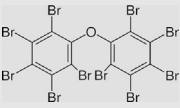
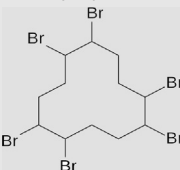
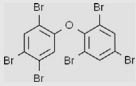
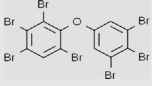
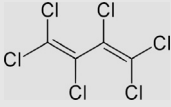
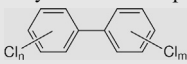
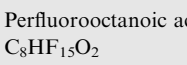

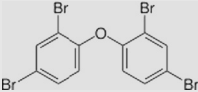
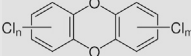
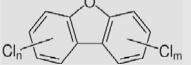
| Name and Chemical structure | Properties | Sources | Toxicity | Environmental Degradation | References |
|--|---|--|---|---|---|
| | Log K_{ow} :5.90 | | Chronic (cumulative) toxicity | atoms. Aerobic biodegradation does not occur readily for toxaphene components with more than 3 chlorine atoms. | (2020) |
| Hexabromobiphenyl $C_{12}H_4Br_6$  | Molecular Weight: 627.6 g/mol Boiling Point:72 °C Melting Point: 246 to 250 °F Solubility: less than 1 mg/mL at 18° C Vapor Pressure: 7.6×10^{-5} mm Hg at 90 °C Log K_{ow} : 6.39 | Use as an additive in flame retardants primarily in thermoplastics | Evidence for Carcinogenicity: EPA: Not evaluated. IARC: Probably carcinogenic to humans | Hexabromobiphenyl is readily degraded in UV light. It is little or no mobility in soil and can volatilize from moist soil surfaces. It is highly persistent under aerobic conditions, but may biodegrade slowly under anaerobic conditions. | (ATSDR, 2004; IARC, 1978; Swann et al., 1983) |
| Decabromodiphenyl ether $C_{12}Br_{10}O$  | Molecular Weight: 959.2 g/mol Boiling Point: 530.0 °C Melting Point: 295.0 °C Solubility: less than 1 mg/mL at 20 °C Density:3.4 Vapor Pressure: less than 1 mm Hg at 20 °C Log K_{ow} : 9.97 | Use as an additive flame retardant for polymers, electronics and electrical equipment. Detected in flue emissions from municipal waste incineration. | Evidence for Carcinogenicity EPA: Not evaluated. IARC: Probably carcinogenic to humans Exposure Routes: The substance can be absorbed into the body by inhalation. | Decabromodiphenyl ether exist solely in the particulate phase in the atmosphere and possibly be removed from the atmosphere by wet or dry deposition. Anaerobic biodegradation of this chemical is very slow. In the absence of sunlight, the compound persists in soils and sediments. | (O'Neil, 2013; IARC, 1999; Wyrzykowska-Ceradini et al., 2011) |
| Hexabromocyclododecane $C_{12}H_{18}Br_6$  | Molecular Weight: 641.7 g/mol Melting point: 179–181 °C α -HBCDD 170–172 °C β -HBCDD 207–209 °C γ -HBCDD Boiling point: Decomposes at > 190 °C Vapour pressure: 6.3×10^{-5} Pa at 21 °C Water solubility: α -HBCDD: 48.8 ± 1.9 μ g/L β -HBCDD: 4.7 ± 0.5 μ g/L γ -HBCDD: 2.1 ± 0.2 μ g/L Log K_{ow} :5.625 | Used as thermal insulation in the building industry, upholstered furniture, automobile interior textiles, car cushions, packaging material, video cassette recorder housing and electric and electronic equipment. | Evidence for Carcinogenicity: No data available Health Effects: The substance is mildly irritating to the eye and it is not irritating to skin. | Slow indirect photochemical degradation with half-life of 3.2 days. Photochemical degradation half-life of 51.2 h. Half-life in aerobic soil is approximately 63 days at 20 °C from sandy loam soil amended with sewage sludge. | (ECHA, 2008) |
| Hexabromodiphenyl ether $C_{12}H_4Br_6O$ | Molecular Weight: 643.6 g/mol Melting Point: | Used as a flame retardant in flexible | Evidence for Carcinogenicity: No data available | Half-life in air is more than 2 days or is subject to | (UNEP, 2007; CEPA, 1999) |

Table 1 (continued)

| Name and Chemical structure | Properties | Sources | Toxicity | Environmental Degradation | References |
|--|---|--|---|--|---|
|  <p>Heptabromodiphenyl ether C₁₂H₃Br₇O</p> | 148–151 °C Boiling Point: 477.4 ± 45.0 °C at 760 mmHg Solubility: 4.08 × 10 ⁻⁶ mg/mL Log K _{ow} : 7.40 Vapour pressure: 6.59 × 10 ⁻⁶ Pa at 21 °C Henry's law constant: 10.6 Pa·m ³ /mol at 25 °C | polyurethane foam | Health Effects: chronic toxicity | atmospheric transport from its source to a remote area. Half-life is more than 182 days in water, more than 365 days in sediment and more than 182 days in soil. | |
|  <p>Hexachlorobutadiene C₄Cl₆ or CCl₂ = CCICCl = CCl₂</p> | Molecular Weight: 260.8 g/mol Boiling Point: 215.0 °C at 760 mm Hg Melting Point: -21.0 °C Solubility: less than 0.1 mg/mL at 22° C Density: 1.675 at 15 °C Vapor Pressure: 0.3 mm Hg at 25° C Log K _{ow} : 4.78 Henry's Law Constant: 0.01 atm·m ³ /mole | Use as flame retardant in the housings of electrical and electronic equipment | Evidence for Carcinogenicity: No data available Health Effects: chronic toxicity | No data for degradation. | (WHO, 1994, Lyman, 1985; EU, 2001) |
|  <p>Polychlorinated biphenyls</p> | Molecular Weight: 414.07 g/mol Boiling Point: 189.0 °C Melting Point: 55.0 °C Solubility: In water, 2290 mg/L at 24 °C | Use as a solvent for elastomers, heat transfer liquid, transformer and hydraulic fluid | Evidence for Carcinogenicity EPA: Possibly carcinogenic to humans. IARC: Not classifiable as to carcinogenicity to humans. Health Effects: irritation eyes, skin, respiratory system, kidney damage. | It may biodegrade in natural waters. The estimated half-lives are 3–30 days in river water and 30–300 days in lake and ground waters. | (Hansch and Leo, 1995 IARC, 1979; Tabak, et al., 1981; Zoeteman et al., 1980) |
|  <p>Perfluorooctanoic acid C₈HF₁₅O₂</p> | Molecular Weight: 414.07 g/mol Boiling Point: 189.0 °C Melting Point: 55.0 °C Solubility: In water, 2290 mg/L at 24 °C | Use as dielectric and coolant fluids in electrical apparatus, carbonless copy paper and in heat transfer fluids. | Evidence for Carcinogenicity: EPA: probable human carcinogens | The half-life in air is during 3.5–7.6 days in air for monochlorobiphenyl to 41.6–83.2 days for pentachlorobiphenyl. Photolysis appears to be the only viable chemical degradation process in water. Biodegradation occurs under both aerobic and anaerobic conditions and is the major degradation process for PCBs in soil and sediment. | (Rossberg et al., 2006) |
|  <p>Perfluorooctanoic acid C₈HF₁₅O₂</p> | Molecular Weight: 414.07 g/mol Boiling Point: 189.0 °C Melting Point: 55.0 °C Solubility: In water, 2290 mg/L at 24 °C | Used worldwide as an industrial surfactant in | Evidence for Carcinogenicity: EPA: Likely to be | Perfluorooctanoic acid is tentative to be resistant to | (Hansen et al., 2001; Moody and Field, 1999; |

(continued on next page)

Table 1 (continued)

| Name and Chemical structure | Properties | Sources | Toxicity | Environmental Degradation | References |
|---|---|---|--|--|--|
|  | Density: 1.792 g/mL at 20 °C Vapor Pressure: 0.53 mmHg Log K_{ow} = 4.81 | chemical processes and as a material feedstock. | carcinogenic to humans. IARC: Carcinogenic to humans. | biodegradation under aerobic or anaerobic conditions. It is possibly resistant to hydrolysis and photolysis. The reported photochemical half-lives in water were 256, > 5000 and > 25,000 years on the ocean surface, open ocean mixing layer and coastal ocean, respectively. | Vaalgamaa et al., 2011 |
| Pentabromodiphenyl ether $C_{12}H_5Br_5O$  | Molecular Weight: 564.7 g/mol Boiling Point: 200–300 °C Melting Point: –5 °C Solubility: Insoluble in water Density: 2.25–2.28 Vapor Pressure: 3.10×10^{-8} mmHg Log Kow: 6.84 | Use as an additive in epoxy resins, phenol resins, polyesters and polyurethane, and textiles. | Evidence for Carcinogenicity: EPA: no studies of cancer in humans exposed Health Effects: Skin and eye Irritation | Half-life for pentabromodiphenyl ether in air is estimated to be 29 days. It is no mobility in soil and it can volatilize from moist soil surfaces. No degradation (as CO_2 evolution) was seen after 29 days. It is expected to adsorb to suspended solids and sediment. | (WHO, 1994, Lyman, 1985; EU, 2001) |
| Polychlorinated dibenzodioxins (PCDDs)  | Boiling Point: higher than 400 °C Solubility: less than 0.1 mg/mL Log K_{ow} : > 6 | PCDDs are the by-products of industrial and combustion processes. | Evidence for Carcinogenicity: IARC: not classifiable as to its carcinogenicity to humans Health effects: diabetes, neurotoxicity, immunotoxicity and chloracne. | PCDDs were expected to have no mobility in soil. It can volatilize from moist soil surfaces. If they are released into water, PCDDs tend to adsorb to suspended solids and sediment. Currently, there is insufficient data for the biodegradation of PCDDs in the environment. | (Hagenmaier et al., 1992; Zubair and Adrees, 2019) |
| Polychlorinated dibenzofurans (PCDFs)  | Melting Point: higher than 150 °C Solubility: less than 0.1 mg/mL Log K_{ow} : > 6 | PCDFs are the by-products of industrial and combustion processes. | Health effects: diabetes, neurotoxicity, immunotoxicity and chloracne. | PCDFs were expected to have no mobility in soil. It can volatilize from moist soil surfaces. If they are released into water, PCDFs tend to adsorb to suspended solids and sediment. The biodegradation of PCDFs in soil is negligible. | (Hagenmaier et al., 1992; Zubair and Adrees, 2019) |

low-cost. Thus, the most promising technologies that could effectively degrade and completely mineralize POPs are photocatalysis (Chong et al., 2010).

In this study, a various of photocatalysts, including TiO₂-based, nano iron-based, metal-organic frameworks (MOFs), porous organic polymer composite, etc., and photocatalytic degradation systems have been favorably prepared and successfully nominated with high-photocatalytic performance. Moreover, reaction conditions, mechanisms, and kinetics for the photodegradation of POPs are also profitably discussed. Prospects and critical challenges related to photodegradation of POPs are also highlighted.

2. Pops background

2.1. Categories of POPs

Persistent organic pollutants (POPs) are toxic organic chemicals that require a very long period of time to degrade under natural conditions in the environment and can accumulate in living organism and ecosystem. POPs have raised significant global concerns due to their persistence in the ecosystem, biomagnification and bioaccumulation in ecosystems, and their significant harmful impacts on human health (Al-Mulali et al., 2015; Bakirtas and Akpolat, 2018) (see Table 1). Consequently, the reduction and elimination of the POPs releasing became the urgent issue in calling the action for the global community. Since 1970s, the use of POPs has been restricted and the release of these compounds has been prohibited in Europe and the USA. From May 2004, these chemicals were listed in the Stockholm Convention with the purpose in terminating or restricting the production and use of this toxic chemical group (Xu et al., 2013). The listed POPs (Fig. 1) in this convention can be placed into 3 categories:

- Pesticides - The majority of chemicals listed in this group are the organochlorine pesticides that have been recognized for their deleterious impacts on the human body and the persistence in the nature. These chemicals are aldrin, chlordane, chlordecone, dicofol, dieldrin, 1,1'-(2,2,2-Trichloroethane-1,1-diyl)bis(4-chlorobenzene) (or DDT), endosulfan and its related isomers, endrin, heptachlor, hexachlorobenzene (HCB), α -hexachlorocyclohexane, β -hexachlorocyclohexane, lindane (or γ -hexachlorocyclohexane), mirex, pentachlorobenzene, pentachlorophenol and its salts and esters, perfluorooctane sulfonyl fluoride, perfluorooctane sulfonic acid and its salts, and toxaphene.
- Industrial chemicals – The chemicals in this group are decabromodiphenyl ether, hexabromobiphenyl, hexabromocyclododecane, hexabromodiphenyl ether and heptabromodiphenyl ether, hexachlorobenzene, hexachlorobutadiene, pentachlorobenzene, PCBs, polychlorinated naphthalenes, perfluorooctanoic acid, its salts and related compounds, short-chain chlorinated paraffins, tetrabromodiphenyl ether and pentabromodiphenyl ether, perfluorooctane sulfonic acid, its salts and perfluorooctane sulfonyl fluoride. The POPs in this category are broadly used in production and manufacturing in industrial processes. For example, PCBs were the chemicals for industrial lubricants and coolants in the production of transformers

and capacitors and other electrical products. Perfluorooctanoic acid has been utilized in producing many consumer goods that resist heat, grease, oil, stains, and water. The release of these POPs was found as environmental contamination in water, soil, and air, as reported in many previous researches (Al-Mulali et al. 2015; Bakirtas and Akpolat 2018).

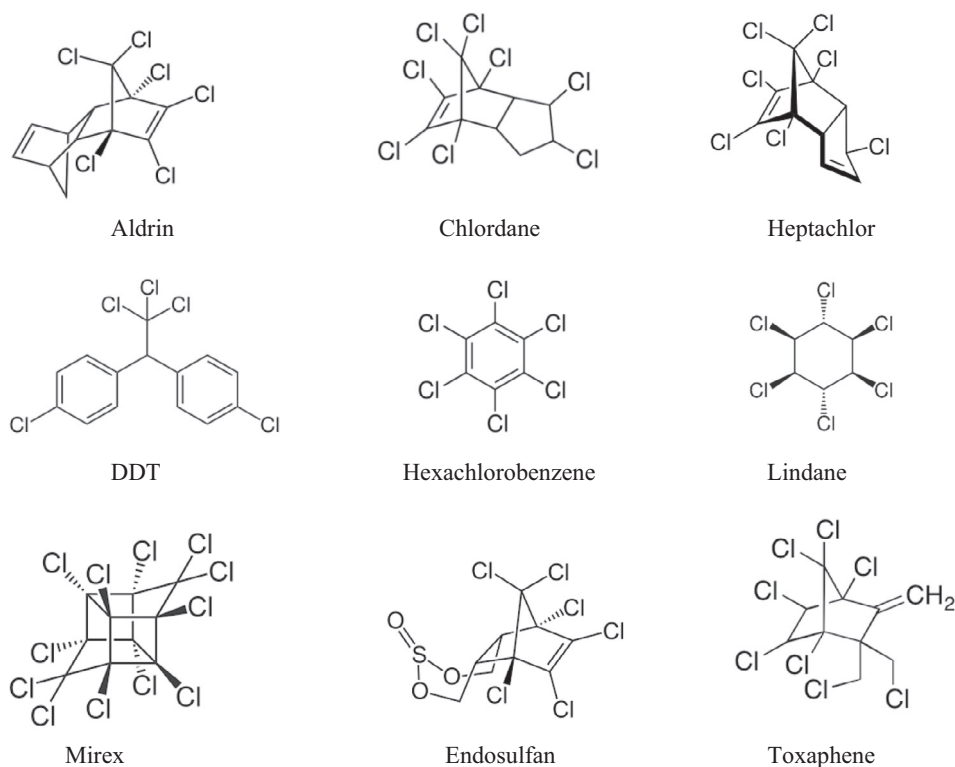
- Unintentional production: These chemicals are the unwanted by-products derived from the chemical or combustion processes that occur in the existence of chlorine compounds. The well-known chemicals in this group are PCBs, PCDDs, and PCDFs. Some other chemicals designated in this group are HCB, hexachlorobutadiene, pentachlorobenzene, and polychlorinated naphthalene. These chemicals should be measured to reduce the unintentional releases to encourage a safe and sustainable environment to the community and ecosystem.

Some listed chemicals such as HCB and pentachlorobenzene were applied as both pesticides and industrial chemicals, while the PCBs were industrial chemicals that were unintentional released from the industrial process. Some new POP chemicals under review by the POPs Review Committee are perfluorohexane sulfonate, dechloran plus, and methoxychlor. The recent emerging pollutants such as some antibiotics such as norfloxacin, carbamazepine, diclofenac, and ibuprofen are also considered as the persistent chemicals (Li et al., 2013; Bu et al., 2016). Their persistent properties are in accordance with the criterion for chemical persistence in water and soil set by United Nations Environmental Program and Canadian Environmental Protection Agency (Bu et al., 2016).

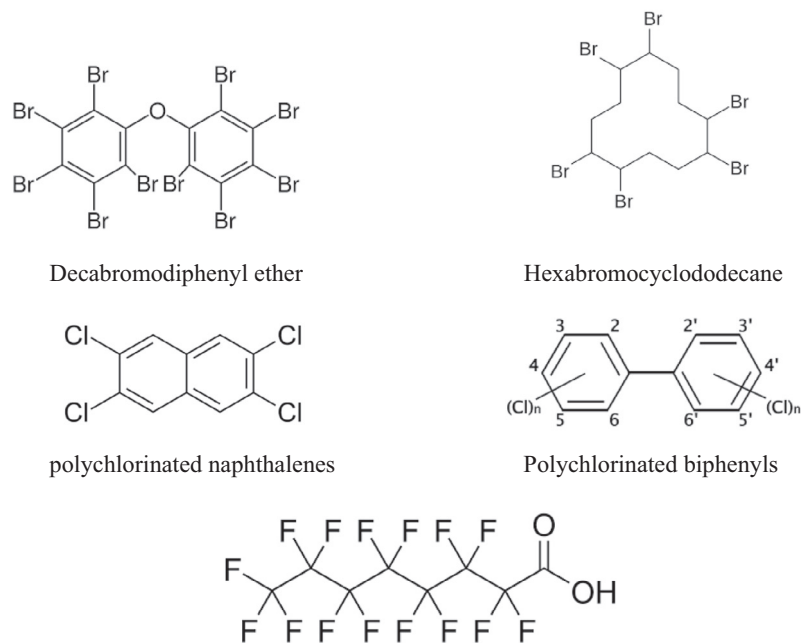
For the last decade, the most common POPs such as DDT, PCBs, PCDDs, and PCDFs have been known for their high toxicity, bioaccumulation potential and are present in massive contamination of the environment (Katsoyiannis and Samara, 2004; Miranda-Garcia et al., 2011; Pariatamy and Kee, 2016). POPs can evaporate into the air, bound to the soil surface, or contaminate in water. However, as the water solubility of POPs is minimal, they tend to gather on solid surfaces such as dust, ash, soil, and sediments. Although POPs are commonly referred as the anthropogenic compounds, their appearance in high concentrations in river and sediments are also reported (Leong et al., 2007; Zakaria et al., 2003). Many previous works reported that the increased risk of cancer, endocrine disruption, neurobehavioral disorders, and reproductive and immune dysfunction could be directed from the exposure of POPs to the human body (Sweetman et al., 2005; Pauwels et al., 2000). Currently, many attempts to remove POPs from the environment using abiotic, biotic, or combination methods have been proposed and reported.

2.2. Conventional methods in POP removal

Owing to a large amount of POPs that have contaminated the environment, such as the air, soil and aquatic systems, (Megharaj et al., 2011) and their toxic properties which can cause a substantial harmful impact on the human health, many research studies have applied several techniques to remove POPs from the ecosystem. A biological process using a wide range of microorganisms is one of the methods commonly used for POP degradation. Due to the abundant nature of microorganisms, and abilities to work in extreme conditions, as well as



(a) Chemical structures of the common pesticides in POPs

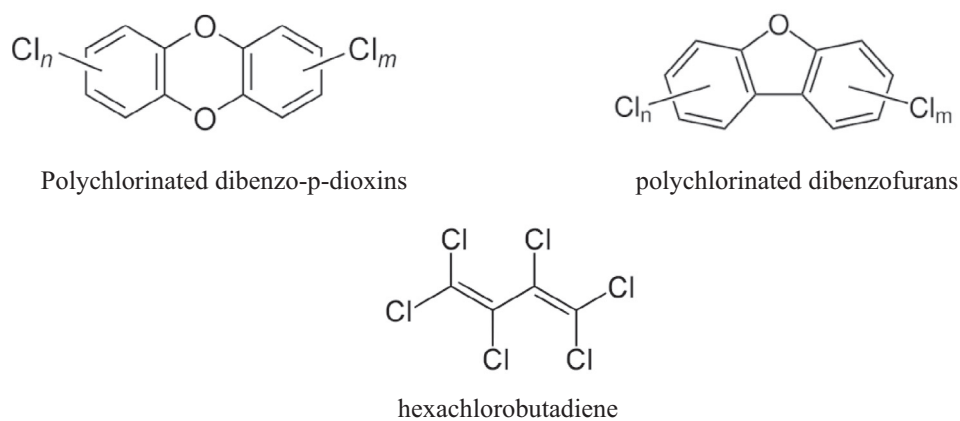


(b) Chemical structures of the common industrial chemicals in POPs

Fig. 1 Chemical structures of some common POPs listed in [Stockholm Convention](#).

having an effective catalytic mechanism and wide diversity, the biological process including bioremediation is often selected for the removal of POPs. [Katsoyiannis and Samara \(2005, 2004\)](#) applied the activated sludge biological process for POPs

degradation and investigated the number of POP chemicals in treated wastewater and solid sludge. Additionally, they found that 65–91% of POPs were degraded in this process depending on the individual species and some POP chemicals could be



(c) Chemical structures of the unintentional POPs from production

Fig. 1 (continued)

mainly destroyed by biodegradation or a biotransformation process. However, 98% of dichlorodiphenyl dichloroethylene was detected in waste sludge while 60% α -hexachlorocyclohexane was remained in treated wastewater. Clara et al. (2005) reported the performance of an activated sludge wastewater treatment and a membrane bioreactor in degrading eight pharmaceuticals, two polycyclic musk fragrances and nine endocrine disruptors. Results showed that both processes did not degrade the antiepileptic drug carbamazepine compounds. In addition, there is an insignificant difference in pollutant removal performance between membrane bioreactor and wastewater treatment processes. Száková et al. (2019) confirmed the accumulation of POPs in sludge collected from wastewater treatment. The contamination of POPs in soil from sewage sludge application such as the polycyclic aromatic hydrocarbons, PCBs, PBDEs, organochlorinated pesticides, perfluorooctane sulfonate, and perfluorooctanoic acid contents was found in the bulk soil. PBDEs, Perfluorooctanoic acid, and Perfluorooctanesulfonic acid contents in soil increased with sludge addition as fertilizer. Ren et al. (2018) also confirmed that organochlorine pesticide, PBDEs, halohydrocarbon, and polycyclic aromatic hydrocarbons as POP components were low degraded by bioremediation in soil because of limitation of bioavailability of POPs. In addition, Wang et al. (2016) studied the HCB biodegradation by using *Typha angustifolia* (*T. angustifolia*) with Hoagland nutrient solution in low (1 mg/L) and high (10 mg/L) concentrations of HCB. The efficiency of HCB degradation showed only about 20% in high concentration and 40% in low concentration for 22 days. The poor microbial capabilities led to the lesser bioavailability of contaminants and the lacking of benchmark values for the testing of bioremediation efficiency were the limitations in using bioremediation in the POPs removal (Megharaj et al., 2011).

As an alternative method besides the biological process, the physico-chemical such as coagulation-flocculation, oxidation, and adsorption have been widely applied to remove POPs from environmental media (Aziz et al., 2007). Alum is a widely chosen coagulant for hydrocarbon compound removal including POPs due to its inexpensive price and easy availability (Renault et al., 2009). However, the working condition with alum is highly dependent on working parameters such as

mixing speed, pH, temperature, retention time, and dosage of coagulant/ flocculants. Linares-Hernández et al. (2010) combined electrocoagulation and electrooxidation processes to treat POPs in industrial wastewater. This combined process can decrease reaction time to less than 2 h, which is better than the electrooxidation process alone that requires a reaction time of more than 21 h. However, the major drawbacks of the coagulation are due to the high price of the chemical coagulants and the large amount of sludge generated from the coagulation-flocculation process (Verma et al., 2012).

Adsorption process is one of the potential methods in POPs removal. The Matériel Institut Lavoisier (MIL) is the most widely used MOFs for this purpose. Phenol, nitro-phenol, ibuprofen drug, trimethoprim, sulfamethoxazole, diclofenac sodium, and aspirin were investigated for the removal efficiency in adsorption process using magnetic porous carbon prepared from MOFs which are Fe-MIL-53 (Tran et al., 2020, 2019a, 2019b), Fe-MIL-88B (Tran et al., 2019c). In addition, tetracycline drug was experimented by using MOFs-templated porous carbon (Tran et al., 2019d), while the chloramphenicol adsorption was applied by using mesoporous carbons preparing from the metal organic framework $Fe_3O_4(BDC)_3$ coated with zero-valent iron particles (Tran et al., 2019e). From the previous researches (Tran et al., 2020, 2019a, 2019b, 2019e), Fe-MIL-53 modified by the pyrolytic process provided the higher adsorption capacity than original MIL-53 more than 4 times for phenol and 5 times for nitrophenol. Fe-MIL-53 removed tetracycline in the water close to 100% and adsorption capacity was about 224 mg/g, which was the highest value compared with other adsorbents. The recyclability of $Fe_3O_4(BDC)_3$ at least 4 times for chloramphenicol adsorption was confirmed, while Fe-MIL-53 was recycled at least 5 times for ibuprofen and 4 times for trimethoprim and sulfamethoxazole. However, the pollutant concentrations, adsorbent doses and pH of solutions exerted the significant effects on adsorption performances.

Membrane technology was also widely applied in water desalination and wastewater treatment processes. Carbon nanotubes (CNTs) based composite membrane was used to filtrate POPs such as triclosan, acetaminophen, and ibuprofen (Ma et al., 2017). They reported that the efficiency (10–90%) was depended on the number of aromatic rings. This process using

CNTs-composite membrane was suitable for low concentrations of POPs owing to the fact that no regeneration is required and the working ability of the membrane in a long period of separation time. Recently, the integration technology of various technologies such as membrane bioreactor (Navaratna et al., 2016), granular activated carbon (Navaratna et al., 2016), the nano-catalysis such as Fe/Pd (Vlotman et al., 2019) with the membrane has been focused. Ametryn removal percentage of combined process between membrane bioreactor and granular activated carbon was about 64% after 12 h, whereas ametryn removal percentage of only biological process was about 83% after 36 h. The catalytic membrane degradation was investigated to remove hexachlorobiphenyl in term of dechlorination efficiency. The observed reaction rate constants increased with increasing the Fe/Pd contents, while the half-time ($t_{1/2}$) of pollutant removal decreased about 10 times compared with membrane without Fe/Pd catalysts. However, the leaching of Fe and Pd was occurred. Lv et al. (Lv et al., 2016) reported the success in destroying the polybrominated diphenyl ethers by sequential methods using anaerobic debromination over nZVI/Pd under nitrogen atmosphere, an oxidation Fenton-like process and an aerobic biodegradation by using *Pseudomonas putida*. Both anaerobic debromination over nZVI/Pd under nitrogen atmosphere and an oxidation Fenton-like process can decompose PBDEs to mono-phenyl-ring compounds and, consequently, the biological process can continuously degrade the pollutants to be CO₂ confirmed by 90% total organic carbon removal for 24 h.

3. Removal of POPs using TiO₂ photocatalysis

3.1. TiO₂ and its modification photocatalysts

Offering many excellent properties, including chemical stability, wide availability, inexpensive, and dependable structure-electronic properties, TiO₂-based photocatalysts are notably considered as the most common materials to destruct POPs. Basically, holes (h^+) and electrons (e^-) could be generated on the surface of the photocatalytic materials (e.g., TiO₂) upon light irradiation ($h\nu \geq E_g$) (Do et al., 2020; Fu et al., 2019).



Therefore, (h^+) and (e^-) may further proceed with water (H₂O) and oxygen (O₂), respectively, to create different types of reactive radicals (for example, hydroxyl radicals (OH \cdot), and active oxygen species (O₂ $^{\cdot-}$)).

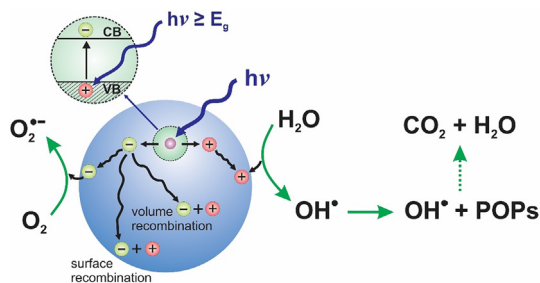


Fig. 2 The general mechanism for photocatalytic removal of persistent organic pollutants (POPs).



Thus, (OH \cdot) hydroxyl radicals will continuously react with POPs for dehalogenation and shortening the chain (C_n → C_{n-1}), with the expected final products of H₂O, carbon dioxide (CO₂) (seen in Fig. 2).

Many types of TiO₂ with different surface properties and crystal structures are widely studied (Tang et al., 2020). Nevertheless, TiO₂ mostly absorbs and operates under the ultraviolet (UV) wavelength region (comprise < 5% of solar terrestrial radiation) because of wide bandgap (3.0–3.2 eV). From a practical perspective, many concepts, such as immobilized TiO₂ on different supports, metal/nonmetal-doping nanoparticles (Choi et al., 1994; Ananpattarachai et al., 2016a; Ananpattarachai et al., 2009; Ananpattarachai et al., 2016b; Umebayashi et al., 2002), hybridizing with the semiconductor materials (Li et al., 2014), hybridizing with the carbonaceous nanomaterials (Fu et al., 2018; Song et al., 2012) and the addition of oxidants (Andersen et al., 2013), etc., are available that could address improving the activity of TiO₂-based photocatalysts. The summary of photodegradation of POPs over various TiO₂ and its modification photocatalysts is listed in Table 2.

3.1.1. Modification of surface properties and crystal structures

Many researchers have modified the crystal structures and surface properties of TiO₂. Many types of commercial and modified-TiO₂ photocatalysts, including commercial Degussa P25 (Dillert et al., 2007; Govindan et al., 2013; Lin and Lin, 2007; Lopes da Silva et al., 2017; Wang and Zhang, 2011), sol-gel TiO₂ (Khan et al., 2014) hydrophobic TiO₂ nanotubes (Tang et al., 2020), TiO₂ nanotubes (Thomas and Chitra, 2014; Tian et al., 2017; Yu et al., 2015), are broadly investigated for photocatalytic degradation by UV light. In most cases, modifying the surface properties and crystal structures of TiO₂ would enhance the activity, compared with bulk TiO₂. For example, Tang et al. developed hydrophobic TiO₂ nanotubes hydrophobic TiO₂ nanotubes, which performed an excellent nanoparticle photocatalyst (Tang et al., 2020). They found that the initial adsorption rate over hydrophobic TiO₂ nanotubes was 4 times higher than that over bare TiO₂ nanotubes, and the apparent rate constant of hydroxyl radicals over hydrophobic TiO₂ nanotubes was 1.8 times higher than that of the hydrophilic TiO₂ nanotubes, leading to the successful selective degradation of pollutant. However, the reaction is mainly performed under the UV region, which is not applicable in practice.

3.1.2. Immobilized TiO₂ on different supports

Several attempts have been made to prevent the numerous disadvantages of TiO₂ in suspension system (such as recovering the suspended TiO₂ powders from the effluent stream, ready for large scale-up photoreactor, etc.) by immobilizing TiO₂ on different supports, including cotton, cotton flax and polyester (Le Cunff et al., 2015), and glass fiber (Le Cunff et al., 2015; Xia et al., 2005), stainless steel (Balasubramanian et al., 2004), polyethylene terephthalate monoliths (Sánchez et al., 2006), sepiolite plates (Suárez et al., 2008), silicate plate (Hewer et al., 2009), glass spheres (Miranda-García et al., 2014), and glass slides (Yu et al., 2007). For example, Le Cunff

Table 2 Summary of the photodegradation of POPs over TiO₂-based photocatalysts.

| No. | Categories | Photocatalysts | POPs | Reaction conditions | Decomposition efficiency (%) | References |
|-----|--|--|--|--|------------------------------|--|
| 1 | TiO ₂ modification of surface properties and crystal structures | Degussa P25 | Perfluorooctanoic acid (PFOA) | UVB (12 W·m ⁻²); T = 25 ± 1 °C; catalyst dose = 1 g·L ⁻¹ ; PFOA = 30 mg·L ⁻¹ ; t = 180 min | 23% | (Lopes da Silva et al., 2017) |
| 2 | | TiO ₂ TNTs | Pentachlorophenol (PCP) | 500 W Xe lamp (100 mW·cm ⁻² ; λ > 400 nm); catalyst dose = 1 g·L ⁻¹ ; PCP = 10 mg·L ⁻¹ ; t = 160 min | 59.4% | (Yu et al., 2015) |
| 3 | Immobilized TiO ₂ on different supports | Si/Ti-2 (two TiO ₂ layers coated on sepiolite plates) | Trichloroethylene (TCE) | UVA fluorescent lamps (365 nm, 4.4 mW·cm ⁻²); the flow of TCE and air gas mixture = 300 mL·min ⁻¹ ; TCE = 90 ppm; | 90% | (Hewer et al., 2009) |
| 4 | | immobilized TiO ₂ /chitosan | terbutylazine (TBA) | TBA = 5 mg·L ⁻¹ ; T = 35 °C; N = 1000 rpm; λ = 254 nm; pH 5; t = 80 min; | 100% | (Le Cunff et al., 2015) |
| 5 | TiO ₂ -doped with the metal/ nonmetal nanoparticles | Ag/TiO ₂ TNTs | PCP | 500 W Xe lamp (100 mW·cm ⁻² ; λ > 400 nm); catalyst dose = 1 g·L ⁻¹ ; PCP = 10 mg·L ⁻¹ ; t = 160 min | 99% | (Yu et al., 2015) |
| 6 | | W/TiO ₂ | Paraquat | sunny day (430 klx); paraquat = 25 ppm; pH 6.5; catalyst dose = 1 g·L ⁻¹ ; t = 180 min | 98% | (Kaur et al., 2019) |
| 7 | | N-F/TiO ₂ | PCP | Suntest XLS + apparatus (Xe lamp, 2.2 kW, 290 < λ < 800 nm, 750 W·m ⁻²); catalyst dose = 0.5 g·L ⁻¹ ; T = 25 °C; PCP = 5 mg·L ⁻¹ ; pH 6.7; t = 120 min | 100% | (Antonopoulou et al., 2015) |
| 8 | | N/TiO ₂ | 1,1,1-trichloro-2,2-bis (p-chlorophenyl) ethane (p,p'-DDT) | 150 W halogen lamp (λ > 420 nm, 14.38 W·m ⁻²); T = 25–31 °C; Acetone: 0.4 wt% in solution; catalyst dose = 1 g·L ⁻¹ ; pH 7; t = 45 min | 100% | (Ananpattarachai and Kajitvichyanukul, 2015) |
| 9 | Coupling with the semiconductor materials | AgInS ₂ /TiO ₂ heterojunction composites | 1,2-dichlorobenzene (o-DCB) | 500 W Xe lamp (λ > 400 nm); catalyst dose = 0.23 g·L ⁻¹ ; o-DCB = 38.5 μL·L ⁻¹ ; Room temperature; | 50% | (Liu et al., 2016) |
| 10 | Hybridizing with the carbonaceous nanomaterials | MWCNTs /TiO ₂ (1:10) | PFOA | 300 W medium pressure Hg lamp (365 nm); catalyst dose = 1.6 g·L ⁻¹ ; PFOA = 30 mg·L ⁻¹ ; T = 23 ± 3 °C; pH 5.0; t = 8 h | 94% | (Song et al., 2012) |
| 11 | | RGO/TiO ₂ NTs | PCP | 500 W Xe arc lamp (100 mW·cm ⁻²); PCP = 10 mg·L ⁻¹ ; pH 8; t = 120 min | 76% | (Zhang et al., 2013) |
| 12 | Hybridizing with the addition of oxidants | TiO ₂ with peroxymonosulfate (PMS, Oxone®) | Atrazine | 300 W Xenon lamp (47.1 mW·cm ⁻² , AM 1.5G); T = 27 ± 3 °C; pH 5.8, 10 mM oxidant; t = 120 min, | 80% | (Andersen et al., 2013) |

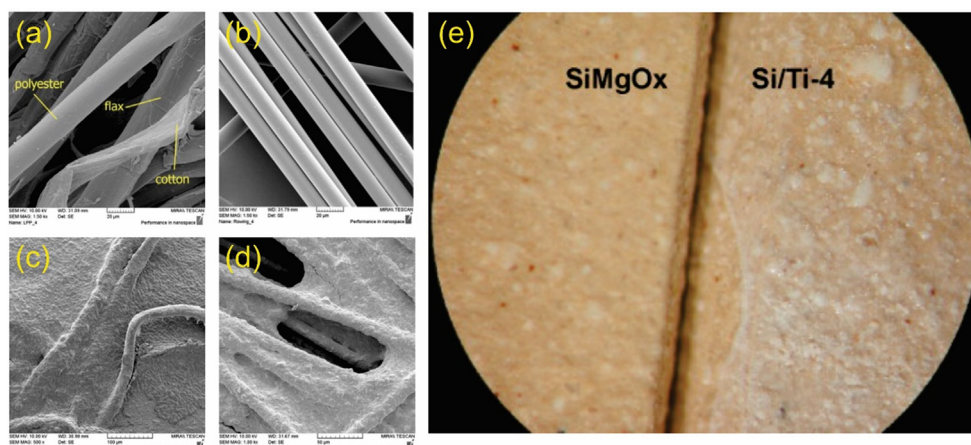


Fig. 3 The SEM micrographs of bulk support materials: (a) cotton/flax/polyester fabric (1500 \times), (b) glass fiber (1500 \times); and fresh TiO₂/chitosan layer supported on the support materials: (c) cotton/flax/polyester fabric (500 \times); (d) glass fiber with catalyst (1000 \times). Adapted with permission from (Le Cunff et al., 2015). (e) The SEM micrograph of bulk and TiO₂-coated silicate plate. Adapted with permission from (Hewer et al., 2009).

et al. successfully dispersed TiO₂/chitosan on cotton, cotton flax, polyester and glass fiber woven for photodegradation of herbicide terbuthylazine (Le Cunff et al., 2015). As observed in Fig. 3(a and b), the bulk supports have an even surface without noticeable imperfections and irregularities. After coating, the surface of supports could be entirely covered by photocatalyst, resulting in the skinny immobilized layer, as seen in Fig. 3(c and d). In another example, the silicate plate was successfully used as support and was fully covered by 4 layers of TiO₂ (as seen in Fig. 3(e)) (Hewer et al., 2009). Although significant efforts have been made, it still requires improving TiO₂ coating layers to have more homogeneity and crystallinity by exploring new methods/techniques.

3.1.3. TiO₂-doped with the metal/nonmetal nanoparticles

The doping technique offers many advantages, including suppressing the recombination of the electron-hole pair, extending to the visible light absorption, which has been intensively investigated. Fig. 4(a and b) illustrated that the metal doping method can create a new donor level above the initial valence band and new acceptor level beneath the initial conduction band, respectively, to apprehend a charge carrier transfer in the visible region (Chen et al., 2010). At the earlier stage of the TiO₂ doping technique, special attention was focused on noble metals, such as Pt (Li et al., 2016), Au (Thomas and Chitra, 2014), Ag (Li et al., 2016; Thomas et al., 2011; Tian et al., 2017; Yu et al., 2015; Zhang et al., 2012), Pd (Li et al., 2016). Following this, other transition metals, including Zn (Sakee and Wanchanthuek, 2017), W (Byrappa et al., 2000; Kaur et al., 2019), and Ni-Cu (Jing et al., 2006), have been investigated for the photodegradation of POPs. After that, other metal systems, including Pb (Chen et al., 2016), Bi₂O₃ (Su et al., 2012), have been of growing interest to researchers. Clearly, bulk TiO₂ exhibits lower activity for the photodegradation of POPs than that of metal-doped candidates. The intense research and development effort have also focused on nonmetal doping, which could extend into the operating range of visible-light-active region via the new valence band (see Fig. 4(c)) (Chen et al., 2010). Hitherto, some studies have been dedicated to this approach, including N-F (Antonopoulou

et al., 2015; Govindan et al., 2013; Samsudin et al., 2015), N (Ananpattarachai and Kajitvichyanukul, 2015), P, F, P-F (Khan et al., 2014), B (Su et al., 2012; Yola et al., 2014), S (Liu et al., 2009). It can be seen that nonmetal-doping not only promotes the stabilization of charge separation, and the effective formation rate of hydroxyl radicals ($\cdot\text{OH}$) (Samsudin et al., 2015), but also improves the TiO₂ particle dispersion, forbidding particle size agglomeration as well as retarding phase transformation (Khan et al., 2014), leading to the enhanced photodegradation of POPs. The summary of photodegradation of POPs by doping technique is listed in Table 3.

3.1.4. Coupling with the semiconductor materials

An intense effort has been focused on developing TiO₂-based photocatalysts by coupling with many candidate semiconductor materials, such as ternary chalcogenide (Cu, Ag)-(Al, In, Ga)-(S, Se, Te), via many methods and techniques. For example, the CuInS₂ modified TiO₂ heterostructure was productively synthesized by an ultrasonication-assisted cathodic electrodeposition method (Li et al., 2014). Clearly, the pure TiO₂ nanotubes performed lower photo-activity for the photodegradation of 2-chlorophenol than that of CuInS₂/TiO₂ nanotubes. In another study, Liu et al. developed AgInS₂/TiO₂ composites by a hydrothermal technique (Liu et al., 2016). The result showed that TiO₂/AgInS₂ heterojunctions exhibited an excellent photocatalytic activity for the photodegradation of 1,2-dichlorobenzene. Their mechanism, which was based on the energy level and electronic traveling, was proposed in Fig. 5 (Liu et al., 2016). Typically, Fig. 5(a) showed the positions of conduction band (CB), valence band (VB) and Fermi level of AgInS₂ and TiO₂, respectively. By fabricating of heterojunction structure, the balanced state for Fermi level of composites would be setup due to the system equilibrium (Hu et al., 2011). Under light irradiation, the photogenerated electrons (e^-) of AgInS₂ would be excited from valence band to conduction band, then it will quickly transfer to the conduction band of TiO₂, as shown in Fig. 5(b). On the one hand, the photogenerated holes (h^+), which remained in the valence band of AgInS₂, could directly react with gaseous

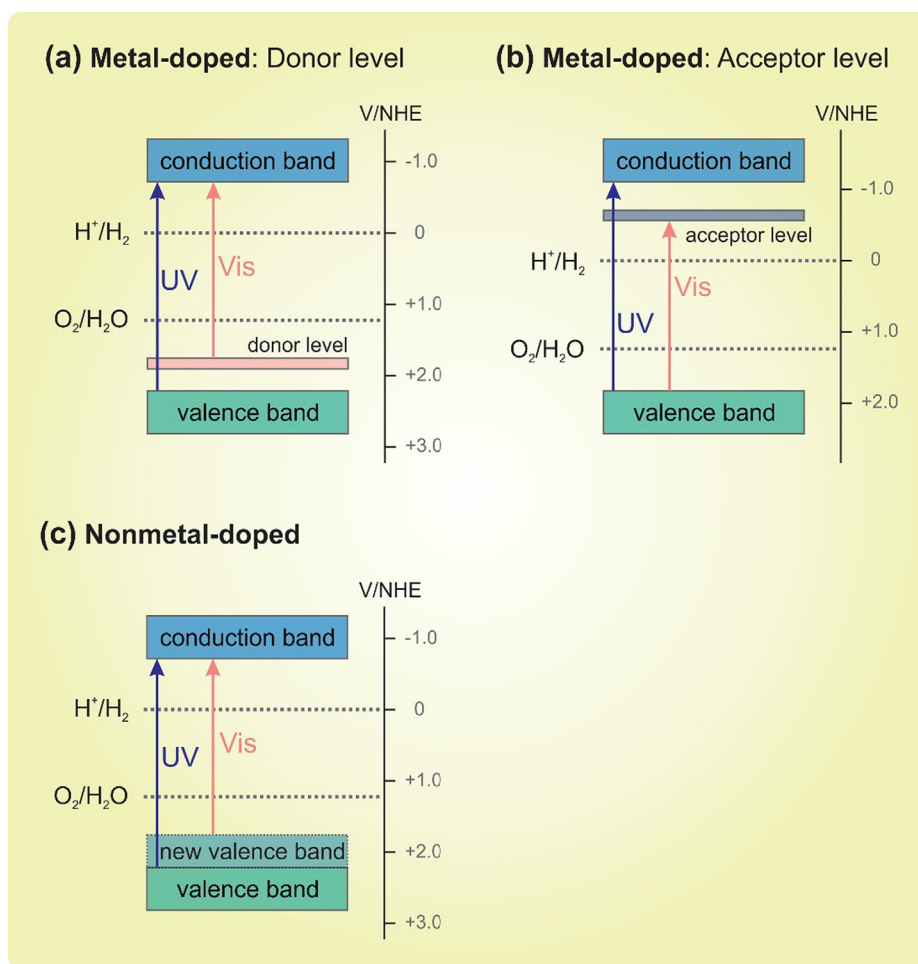


Fig. 4 The metal doping: (a) Donor and (b) acceptor levels; (c) The nonmetal doping: new valence band. Adapted with permission from (Chen et al., 2010); Copyright (2010) American Chemical Society.

1,2-dichlorobenzene to generate different types of products. On the other hand, (e^-) would continually travel and reduce, mineralize 1,2-dichlorobenzene to form other products. The enhancement might be attributed to the depressing of the photo-generated charges recombination in the $\text{TiO}_2/\text{AgInS}_2$ hetero-junction composites.

3.1.5. Hybridizing with the carbonaceous nanomaterials

In another approach, successful attempts have been made to the carbonaceous nanomaterials, including CNTs, multi-walled carbon nanotubes (MWCNTs), fullerene, and graphene nanosheets, etc. They have been dedicated as notable supports: (a) long lifetime in term of electron-hole separation (Yao et al., 2008), (b) outstanding adsorption of reactants (Velasco et al., 2010), and (c) excellent physical properties (large BET surface area, and high electron mobility) (Panchangam et al., 2018). For example, $\text{TiO}_2/\text{MWCNT}$ photocatalysts, which were synthesized by the sol-gel technique, displayed an excellent photodegradation of perfluorooctanoic acid (Song et al., 2012), dimethyl phthalate esters (Tan et al., 2018), 2,6-dinitro-p-cresol (Wang et al., 2009). The presence of MWCNT in TiO_2 promotes to facilitate the generation of reactive radicals via transforming the photo-generated electrons into the TiO_2 conduction band, leading to the enhancement of photocatalytic degradation of POPs. In another approach, several TiO_2 -

graphene nanocomposites were also developed for the photodegradation of aldicarb, and norfloxacin (Li et al., 2013), perfluorooctanoic acid (Gomez-Ruiz et al., 2018; Panchangam et al., 2018). They found that the combination of reduced graphene oxide (rGO) and TiO_2 (so called (rGO)- TiO_2) exhibited a superior photocatalytic performance, up to 99.2% of removal perfluorooctanoic acid efficiency for 8 h by UV-C irradiation (8 W, 254 nm) (Panchangam et al., 2018) and $93 \pm 7\%$ of removal perfluorooctanoic acid efficiency for 12 h by UV-vis light (Hg lamp, 200–600 nm) (Gomez-Ruiz et al., 2018). Zhang et al. found that rGO/ TiO_2 NTs could reach to 76% in photodegradation of pentachlorophenol (Zhang et al., 2012). In another example, the combination of graphene oxide (GO) and other catalysts in form of GO- TiO_2 - $\text{Sr}(\text{OH})_2/\text{SrCO}_3$ material was prepared and favored the photocatalytic degradation of phenanthrene (and potentially other POPs) in complex water matrices using simulated solar light (Fu et al., 2018). There are two factors, including (a) hybrid coupling TiO_2 - $\text{Sr}(\text{OH})_2/\text{SrCO}_3$ and (b) effective electron transfer in graphene oxide sheets, could be attributed to this enhancement.

3.1.6. Hybridizing with the addition of oxidants

There is another possible approach to extend range under visible light, namely hybridizing with the addition of oxidants into the

Table 3 Summary of the photodegradation of POPs over TiO₂-doped with the metal/nonmetal nanoparticles.

| No. | Photocatalysts | POPs | Reaction conditions | Decomposition efficiency (%) | References | |
|-----|----------------------------------|--|---|--|-------------------|--|
| 1 | Noble metals | Pt/TiO ₂ | 125 W high-pressure Hg lamp (365 nm, light intensity 5.3 mW·cm ⁻²); catalyst dose = 0.5 g·L ⁻¹ ; PFOA = 60 mg·L ⁻¹ ; pH 3.0; air flow = 60 mL·min ⁻¹ ; t = 7 h | 100% | (Li et al., 2016) | |
| 2 | | Pd/TiO ₂ | | 94.2% | | |
| 3 | | Ag/TiO ₂ | | 57.7% | | |
| 4 | | Ag/TiO ₂ | Pentachlorophenol (PCP) | UV light (UV-A, 365 nm); catalyst dose = 0.125 g·L ⁻¹ ; PCP = 20 mg·L ⁻¹ ; t = 160 min | 98% | (Zhang et al., 2012) |
| 5 | | Ag/TiO ₂ | PCP | 500 W Xe lamp (100 mW·cm ⁻² ; λ > 400 nm); catalyst dose = 1 g·L ⁻¹ ; PCP = 10 mg·L ⁻¹ ; t = 160 min | 99% | (Yu et al., 2015) |
| 6 | Transition metals | Zn/TiO ₂ | Paraquat | 11 W UV lamp (8 lamps, 160 mA); catalyst dose = 4 g·L ⁻¹ ; paraquat = 400 ppm; pH 7.0; t = 360 min | 80% | (Sakee and Wanchanthuek, 2017) |
| 7 | | W/TiO ₂ | Paraquat | sunny day (430 klx); paraquat = 25 ppm; pH 6.5; catalyst dose = 1 g·L ⁻¹ ; t = 180 min | 98% | |
| 8 | | Ni-Cu/TiO ₂ | PFOA | 23 W low-pressure Hg lamp (254 nm); PFOA = 25 mg·L ⁻¹ ; t = 360 min | 100% | (Jing et al., 2006) |
| 9 | Other metals | Pb/TiO ₂ | PFOA | 400 W UV lamp (254 nm); catalyst dose = 0.5 g·L ⁻¹ ; pH 5; 298 K; PFOA = 50 mg·L ⁻¹ ; t = 12 h | 99.9% | (Chen et al., 2016) |
| 10 | | Bi ₂ O ₃ /TiO ₂ | PCP | a 500 W tungsten halogen lamp (λ > 420 nm); PCP = 10 mg·L ⁻¹ ; catalyst dose = 1 g·L ⁻¹ ; t = 5 h | 10% | (Su et al., 2012) |
| 11 | Nonmetals | N-F/TiO ₂ | Atrazine (ATR) | UV lamp (6–20 W, λ = 350 nm); catalyst dose = 0.5 g·L ⁻¹ ; ATR = 2 mg·L ⁻¹ ; t = 360 min | 46% | (Samsudin et al., 2015) |
| 12 | | N-F/TiO ₂ | PCP | Suntest XLS + apparatus (Xe lamp, 2.2 kW, 290 < λ < 800 nm, 750 W·m ⁻²); catalyst dose = 0.5 g·L ⁻¹ ; T = 25 °C; PCP = 5 mg·L ⁻¹ ; pH 6.7; t = 120 min | 100% | (Antonopoulou et al., 2015) |
| 13 | | N/TiO ₂ | 1,1,1-trichloro-2,2-bis(p-chlorophenyl)ethane (p,p'-DDT) | 150 W halogen lamp (λ > 420 nm, 14.38 W·m ⁻²); T = 25–31 °C; Acetone: 0.4 wt % in solution; catalyst dose = 1 g·L ⁻¹ ; pH 7; t = 45 min | 100% | (Ananpattarachai and Kajitvichyanukul, 2015) |
| 14 | | P/TiO ₂ | ATR | 15 W fluorescent lamp (2 lamps, 315–700 nm, 0.095 mW·cm ⁻²); ATR = 2.32 μM (0.5 mg·L ⁻¹); pH 3; catalyst dose = 0.5 g·L ⁻¹ ; t = 6 h | 71% | (Khan et al., 2014) |
| 15 | | F/TiO ₂ | ATR | | 49% | |
| 16 | | P-F/TiO ₂ | ATR | | 81% | |
| 17 | | B/TiO ₂ (TiO ₂ -BEW) | ATR | 400 W UV lamp (λ = 250–570 nm); ATR = 10 mg·L ⁻¹ ; catalyst dose = 1.5 g·L ⁻¹ ; t = 70 min | 83% | (Yola et al., 2014) |
| 18 | | TiO _{2-x} B _x | PCP | a 500 W tungsten halogen lamp (λ > 420 nm); PCP = 10 mg·L ⁻¹ ; catalyst dose = 1 g·L ⁻¹ ; t = 5 h | 40% | (Su et al., 2012) |
| 19 | | S/TiO ₂ | ATR | Solar light (experiment time was at 11:10–11:40 every day, 16 μW·cm ⁻²); ATR = 50 μg·L ⁻¹ ; t = 30 min | 68.6% | (Liu et al., 2009) |
| 20 | Metal-nonmetal hybrids and other | La-B/TiO ₂ | PCP | Solar light (experiment time was at 14:00–16:00 in May, 27.5–39.0 μW·cm ⁻²); PCP = 0.0181 mM; catalyst dose = 0.4 g·L ⁻¹ ; pH 5.7 ± 0.1; t = 120 min | 81% | (Liu et al., 2011) |
| 21 | | CdS/TiO ₂ | 1,2,4-trichlorobenzene (1,2,4-TCB) | 240 W Hg-quartz lamp (λ = 240–320 nm); T = 34 ± 1 °C; 1,2,4-TCB = 0.1 mol·L ⁻¹ ; air flow = 2.5 L·min ⁻¹ ; 50 mL MeOH; t = 100 h | 97.3% | |
| 22 | | ZnSe/TiO ₂ | PCP | 300 W Xe lamp (100 mW·cm ⁻² AM 1.5G); PCP = 10 mg·L ⁻¹ ; catalyst dose = 1 g·L ⁻¹ ; pH 5; t = 120 min | 71% | (ThanhThuy et al., 2013) |

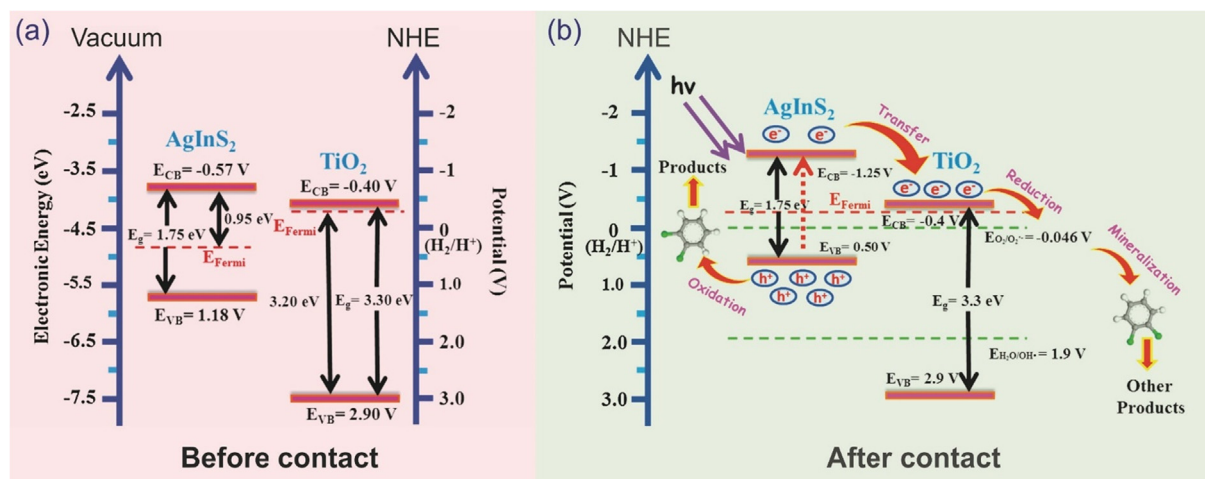


Fig. 5 Proposed energy level and possible electronic traveling for (a) before contact: single nanostructure of TiO_2 and AgInS_2 , and (b) after contact: heterojunction nanostructure of $\text{AgInS}_2/\text{TiO}_2$ (Liu et al., 2016).

system. In a previous study, peroxymonosulfate and persulfate are suggested to be the most promising candidates (Andersen et al., 2013). They could provide effectively sufficient irradiance (UV and/or heat), which leads to generating reactive radical species. As expected, Andersen et al. observed synergic effects by combining TiO_2 with oxidants (such as peroxymonosulfate and persulfate) to generate a significant number of reactive radicals, leading to an enhanced photodegradation rate.

3.2. Operating conditions, kinetics, and performance in POP removal using TiO_2 photocatalyst

3.2.1. Effect of POP properties and concentration on the photocatalytic degradation

Generally, the pollutant degradation in environmental media such as water and soil is mainly relied on their properties and the ability of treatment process. POPs are commonly semi-volatile and slowly evaporate in the air, but can travel in long distance in the atmosphere. With water-immiscible property but high lipid solubility, POPs are not frequently found as water contaminant, but they are easily found in fat and oils. Some types of POPs such as PBDE209 are well disperse as nano-scale particles in atmosphere (Zhang et al., 2016) and easily dissolve in organic solvents such as methanol and tetrahydrofuran (Hardy, 2002; Bastos et al., 2009; Eriksson et al., 2004; Zhao et al., 2009; Bastos et al., 2008). Zhang et al. (2016) reported that degradation of decabromodiphenyl ether in water is possible using photocatalytic process. In water, the degradation of decabromodiphenyl ether in photocatalytic process followed first order kinetics. However, in tetrahydrofuran organic solvent, the decabromodiphenyl ether photocatalytic kinetics followed second-order pattern (Zhang et al., 2016). The rate of decabromodiphenyl ether degradation in tetrahydrofuran was comparatively high with less than 50% of the final debromination which is much lower than that in the pure water. The degradation performance of POPs using photocatalytic degradation is largely reliant on the characteristics of that compound.

The number of chlorine atoms in POPs also plays as a critical factor in photocatalytic removal using TiO_2 . The decrease-

ing in degradation rate of POPs such as PCDDs and PCDFs was inversely proportional to the increasing of chlorines in their molecular structure. Muto et al. (2001) reported that the degradation efficiencies of PCDDs and PCDFs were more than 70% after 24 h in photocatalytic system with the half lives of both compounds in the range 7.92×10^{-2} –0.1 d. The degradation rate of both POPs was largely depended on the chlorination level of PCDDs and PCDFs. Wu et al. (2005) also found that approximately 99% conversion of 1,2,3,6,7,8-hexa chlorodibenzo-P-dioxin and 2,3,7,8-tetrachlorodibenzodioxin were detected when the photocatalytic degradation rate of PCDDs and PCDFs decreased and the chlorination level increased. Moreover, no 2,3,7,8-substituted congener derived from the process were detected. Friesen et al. (1996) and Wu and Ng (2008) reported that the low chlorinated PCDDs and PCDFs was slower degraded than the high chlorinated ones due to the sequential photocatalytic dechlorination of highly chlorinated congeners of POPs. Choi et al. (2000) found that the photocatalysis of PCDDs were followed the first-order kinetics and the degradation rates decreased with the increasing of chlorine atom numbers. The rates also increased with the increasing of light intensity and TiO_2 coating mass. In summary, the photocatalytic degradation rate of POPs was greatly decreased by the chlorination level of the congeners (Kim and O'Keefe, 2000; Choi et al., 2000).

The initial concentration of POPs is also a major factor that affected the degradation performance in photocatalytic process. With the high concentration of POPs, the TiO_2 active sites were shielded with the pollutant compounds and the distance of photons crossing the solution for photocatalytic reaction decreased. In contrast, at low concentrations, the number of charge carriers (e^- and h^+) developed on the TiO_2 surface increased and, consequently, the high amount of the generated hydroxyl radicals can react and remove the POPs in the photocatalytic system. For example, it was reported (Ananpattarachai and Kajitvichyanukul, 2015) that the reaction rate of the parent molecule, r , and the apparent first-order rate constant, k_{obs} , at low concentration of p,p'-DDT was higher than that obtained at a high concentration owing to the increasing of the hydroxyl radicals attacking the investigated pollutants.

3.2.2. Effect of UV or visible light irradiation

The influence of UV irradiation on photocatalysis degradation of the POPs using TiO₂ has been widely investigated and reported. The photolysis (irradiation without TiO₂) or photochemical degradation of POPs was relatively negligible compared to their photocatalytic degradation. For example, [Doll and Frimmel \(2003\)](#) reported that TiO₂ degradation rate constant (*k*) using Hombikat UV100 was approximately 500 times of that using UV light. [Yu et al. \(2007\)](#) conducted the photocatalytic oxidation of organochlorine pesticides such as cypermethrin, dicofol, benzene hexachloride, and the whole efficiency in POPs removal using photocatalysis is much higher than the direct photolysis under the same conditions. Within 10 min irradiation, less than 50% of α -benzene hexachloride, β -benzene hexachloride, δ -benzene hexachloride, and dicofol were remained in the presence of TiO₂, but more than 90% of those corresponding chemicals in the absence of TiO₂ were detected. Apparently, the irradiation is the major factor for the degradation of POPs in photocatalysis system.

The types of irradiation and intensity has a strong impact on the efficiency of POP removal ([Zhao et al., 2004](#); [Ananpattarachai and Kajitvichyanukul, 2015](#)). [Ananpattarachai and Kajitvichyanukul \(2015\)](#) applied different types of lights including UV light, visible light, and simulated solar light for photocatalytic degradation of p,p'-DDT using interstitial N-doped TiO₂. By enhancing UV intensity, more e⁻ and h⁺ can be generated and, consequently, a higher amount of p,p'-DDT compounds could be promptly degraded. Using the visible light, the reaction rate enhancement in the degradation of DDT under the visible light irradiation was nearly five fold higher than that under the UV light irradiation. Comparatively, the simulated solar light gave the highest oxidation rate, corresponded the pseudo-first-order pattern, with the oxidation rate (*r*) of the DDT as 0.859 mg/L-min and the rate constant, *k*_{obs}, as 0.1565 min⁻¹ ([Ananpattarachai and Kajitvichyanukul, 2015](#)). Apparently, the light intension and the light source selection can greatly enhance the reaction rate and performance for POPs degradation.

3.2.3. Effect of catalyst and catalyst loading

The selection of a catalyst is a basis aspect in photocatalysis to obtain a high efficiency in degradation of the toxic compounds

including POPs. [Wu et al. \(2004\)](#) investigated the degradation of 1,2,3,6,7,8-hexachlorodibenzo-P-dioxin and octachlorodibenzodioxin under photocatalysis process using UV light in the combination with three different catalysts, TiO₂, ZnO and SnO₂, immobilized on quartz. It was found that the UV/TiO₂ provided the highest rate constants among the immobilized catalyst in the photodegradation of POPs, while the UV/SnO₂ exerted the lowest rate values. With high efficiency in photocatalytic degradation, TiO₂ is usually the chosen catalyst for POPs removal.

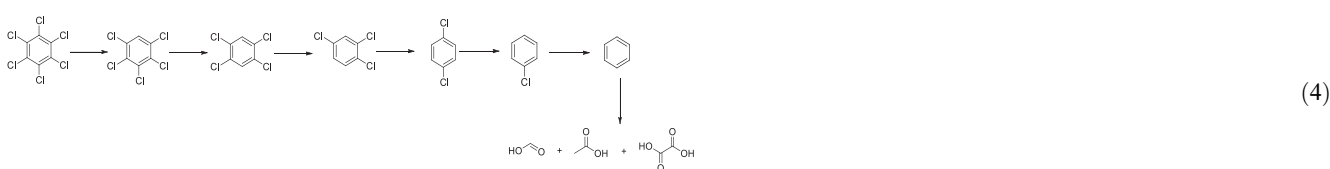
[Wang et al \(2019\)](#) reported the effectiveness of the metal doped TiO₂ systems (i.e., Ag/TiO₂, Pt/TiO₂, Pd/TiO₂, and Cu/TiO₂) in the photocatalytic of PBDEs under UV light. The degradation of 2,2',4',4'-tetrabromodiphenyl ether can achieve high performance with the application of the noble metal doped TiO₂. The hydrogenation experiment from Wang's group suggested that the photocatalytic mechanism of 2,2',4',4'-tetrabromodiphenyl ether in Pd/TiO₂ and Pt/TiO₂ systems was a direct H-atom transfer, while the electron transfer is a key mechanism in Ag/TiO₂ and Cu/TiO₂ systems. Thus, different types of catalyst can lead to a different mechanism in POP removal by photocatalytic process.

Besides the type of the catalyst, the TiO₂ loading is also the important factor affecting photocatalytic removal performance using suspended TiO₂. [Shaban et al. \(2016\)](#) stated that the multiplying of catalyst to the photocatalytic system from 0.25 to 0.5 g/L led to the generating of higher amount of hydroxyl radicals that can enhance the PCB degradation rate in an aqueous solution. However, the increasing catalyst loading also directed to the agglomeration of catalysts in addition to the light shielding by the suspension causing a reduction of the pollutant degradation rate in pollutant removal ([Wang et al., 2019](#)).

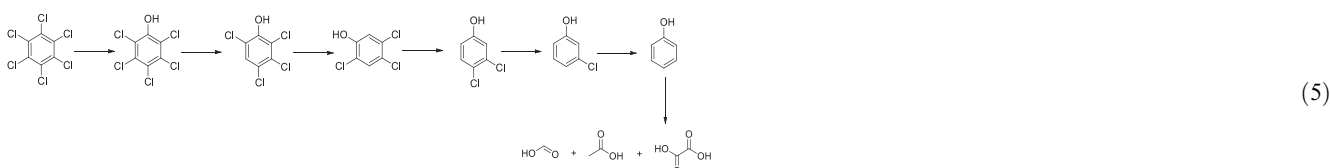
3.2.4. Photocatalytic degradation pathway of POPs

Photocatalytic degradation of hexachlorobenzene was depicted into two pathways, reductive and oxidative dechlorination followed by oxidative ring-opening reactions to give small organic acids and alcohols which are, later, mineralized to CO₂ and H₂O.

Reductive dechlorination:



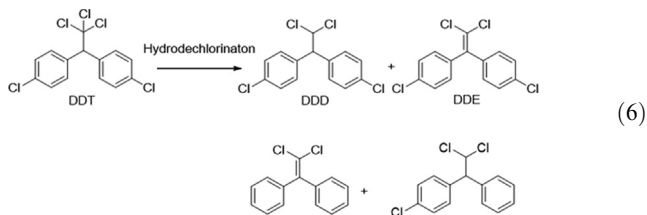
Oxidative dechlorination:



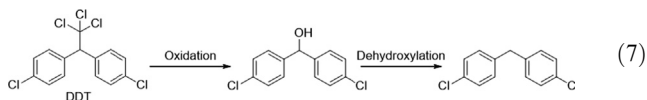
The reductive dechlorination (hydrodechlorination) occurred in the presence of electron donors (hole scavengers) such as water, alcohol in the media (Choi and Hoffmann, 1995; Xia et al., 2015).

Similarly, degradation of DDT under photocatalytic treatments underwent in two major initial pathways, reduction and oxidation (Llompert et al., 2003; Zaleska et al., 2000). The intermediates and degradation pathway for DDT is given as follows.

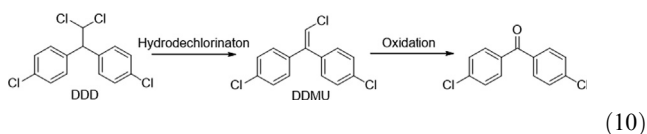
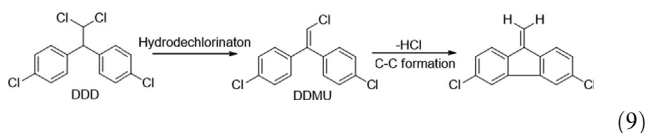
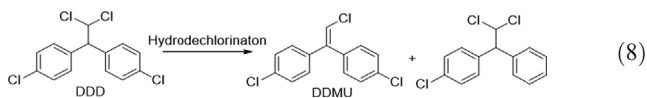
Reductive dechlorination:



Oxidative dechlorination:



Intermediates:

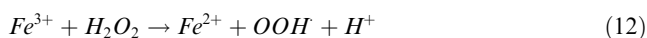
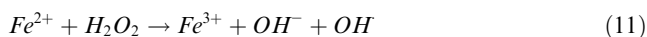


Further detoxification of intermediate species occurred through oxidative ring-opening reactions generally resulted in mineralization.

4. Removal of POPs using Fenton and photo-Fenton reactions

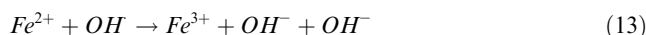
4.1. Removal of POP using Fenton reagent and performance of the system

In 1894, H.J.H. Fenton discovered that hydrogen peroxide reacted with ferrous ions generating hydroxyl radicals which then oxidized with organic contaminants and became known as the Fenton reaction. The Fenton reaction is widely accepted as having high efficiency and a short reaction time to degrade organic pollutants, which affect the microorganism in the biological degradation process. The hydroxyl radical is formed by a reaction between ferrous ions (Fe^{2+}) and hydrogen peroxide (H_2O_2) following Eqs. (11) and (12)

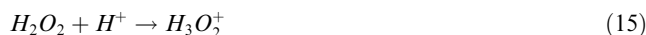


Hydroxyl radicals can oxidize with various organic compounds because these radicals have a strong oxidizing potential ($E^\circ = 2.8$ V) to decompose organic compounds to small molecules.

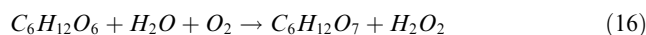
Borba et al. (2018) examined the treatment of tannery effluent (TE) by using the conventional Fenton process. The effects of initial pH of the solution from acid to neutral, as well as, the H_2O_2 and Fe^{2+} concentrations to the performance of Fenton processes are described. The results presented that a decreased initial solution pH and an increased H_2O_2 concentration promoted higher activity of chemical oxygen demand removal. However, the excess of H_2O_2 and Fe^{2+} concentrations beyond the above mentioned can significantly reduce the number of hydroxyl radicals, which might be due to the excessive H_2O_2 and Fe^{2+} ions, as shown in Eqs. (13) and (14).



The initial solution pH is also crucial factor and the suitable condition of the initial pH should be below 4.0. The prohibition of hydroxyl radicals can be observed at a pH solution higher than 4.0 because H_2O_2 can be transformed to $H_3O_2^+$ following Eq. (15)



Ma et al. (2020) studied 2,2,5-trichlorodiphenyl degradation using the Fenton process by examining the effects of various independent parameters i.e. the pH of the solution, reaction temperature, and inorganic ions on 2,2,5-trichlorodiphenyl decomposition. They found that the addition of 50 mM of isopropanol used as a scavenger in Fenton reaction at pH 5.0 inhibited the performance of 2,2,5-trichlorodiphenyl degradation, whereas adding 5 mM of chloroform did not affect the efficiency of 2,2,5-trichlorodiphenyl decomposition. Additionally, Kahoush et al. (2018) studied the H_2O_2 generation by using the enzyme glucose oxidase, as shown in Eq. (16).

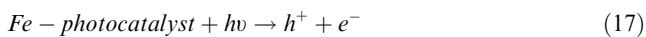


Due to the presence of Fe^{2+} ions, the reaction between Fe^{2+} ions and H_2O_2 was obvious, thus called bio-Fenton, and has been used to degrade many kinds of POPs such as dyes and herbicide. They confirmed that, to achieve a high performance in using the bio-Fenton process, the significant operating variables are the initial solution pH, reaction temperature, initial pollutant concentration and biocatalyst.

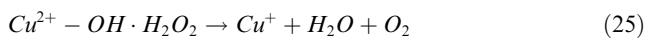
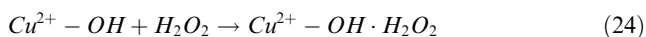
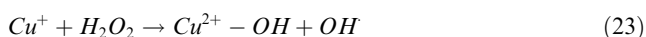
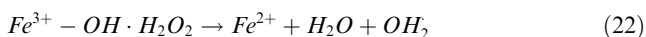
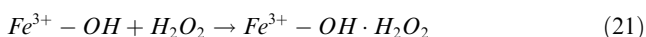
4.2. Removal of POPs using Fenton-like reaction

Nowadays, the persulfate oxidant compound has also been used as a precursor of radicals in Fenton-like reactions in some reports (Avetta et al., 2015; Deng et al., 2014; Li et al., 2015). Wang and Wang (2018) studied trimethoprim degradation by the comparison of efficiency with Fenton and Fe^{2+} -activated persulfate processes. The conventional Fenton process showed higher degradation than the Fe^{2+} -activated persulfate process. On the contrary, the total organic carbons had higher removal by using persulfate than hydrogen peroxide. The efficiency of Fenton-like reactions by using iron in a solid form relied on the initial solution pH. Therefore, the couples between iron

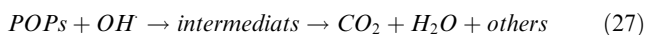
and a photocatalyst can enhance the performance of a Fenton-like reaction by the high production of radicals and the reaction can take place in a neutral pH solution as shown in Eqs. (17)–(20) (Guo et al., 2020; Yang et al., 2020).



Recently, copper (Cu) has been used to improve the proficiency of iron in the Fenton-like process to degrade *p*-cresol pollutants (Wantala et al., 2019). It has been demonstrated that the demineralization of *p*-cresol showed about 80% removal. The reaction between the solid Cu ($\equiv Cu^+$, $\equiv Cu^{2+}$) and iron with oxidants is displayed in Eqs. (21)–(26).



The radicals produced by a Fenton reaction can continuously react with POP chemicals to destroy to small molecules and then to CO₂ and water called green products following Eq. (27).



Currently, many researchers are interested to solve both problems by using iron catalysts in a solid form in a Fenton-like reaction process such as Fe³⁺ impregnated N doped-TiO₂ (Abdelhaleem and Chu, 2020), FeOOH/Bi₂WO₆ (Guo et al., 2020), Fe³⁺-doped BiOBr (Liu et al., 2020), iron-containing RH-MCM-41 (Wantala et al., 2015) and Fe-Cu/NaPI (Wantala et al., 2019) to degrade organic pollutants (carbofuran, methylene blue, rhodamine B, tetracycline hydrochloride, *p*-nitrophenol, reactive red 3 and *p*-cresol). They confirmed that the Fenton-like process was enhanced by photolysis called the photo-Fenton-like process (Abdelhaleem and Chu, 2020; Guo et al., 2020; Liu et al., 2020; Wantala et al., 2015; Yang et al., 2020). The reaction mechanism is exhibited in Eq. (28).



Accordingly, ferrous reacts with oxidants (H₂O₂) to produce hydroxyl radicals and lead to the oxidation reaction in degrading the pollutant.

4.3. Removal of POPs using Photo-Fenton reactions

Many researchers modified the process to transform Fe³⁺ to Fe²⁺ form by photolysis called photo-Fenton reaction (Davididou et al., 2019; Tarkwa et al., 2019; Vergura et al.,

2019). The reduction reaction of Fe³⁺ to Fe²⁺ form is previously presented in Eq. (28).

The POPs were used as pollutants in the photo-Fenton process such as pentachlorophenol (Vergura et al., 2019), and Orange G dye (Tarkwa et al., 2019). They reported that a suitable pH solution was at about 2.8. Garcia-Segura et al. (Garcia-Segura et al., 2017) studied *o*-toluidine degradation by the electro-assisted photo-Fenton process. They found that the ratio of H₂O₂:Fe²⁺ (5:1) in the electro-assisted photo-Fenton process was lower than the conventional Fenton process (20:1) because a faster electro-regeneration of the iron catalyst occurred following Eq. (29).



Furthermore, H₂O₂ was generated by oxygen reduction at the cathode (Eq. (30)) and oxidation at the anode (Eq. (31)), respectively, in an acidic condition of electro-Fenton reaction.

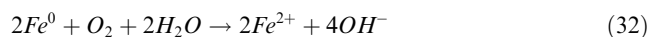


However, using the homogenous Fenton, electro-Fenton and photo-Fenton reactions to degrade POPs have to be set in acid conditions (pH 2–4), which is the main disadvantage of the process. Additionally, the formations of iron sludge after the reaction is a weakness of this process as well.

Katsumata et al. (2006) also reported degradation of PCDDs. PCDDs, including tetra- to octa-chlorinated dibenzo-*p*-dioxin were dissolved in water and degraded by photo-Fenton process. Under optimum Fe²⁺ and H₂O₂ concentrations, the complete removal of 2,3,7,8-tetra-chlorinated dibenzo-*p*-dioxin was achieved after 20 min. The tetra-chlorinated dibenzo-*p*-dioxin, penta-chlorinated dibenzo-*p*-dioxin and hexa-chlorinated dibenzo-*p*-dioxin were completely degraded in 120 min. However, hepta-chlorinated dibenzo-*p*-dioxin and octa-chlorinated dibenzo-*p*-dioxin were still detected even after 300 min. The degradation rates of the POPs decreased as the chlorine substituents increased as reported by Kim and O'Keefe (2000).

4.4. Removal of POPs using zero valent irons (ZVI)

Zero valent irons (ZVI) and nano zero-valent irons (nZVI) were used as iron sources in the Fenton reaction (Correia de Velosa and Pupo Nogueira, 2013; Deng et al., 2014; Graça et al., 2018; Tian et al., 2020). The oxidation of ZVI and nZVI was converted to Fe²⁺, as shown in Eq. (32) and Fe³⁺ was recycled back to Fe²⁺ following Eq. (33).



Then, Fe²⁺ reacted with H₂O₂ to produce hydroxyl radicals following Eq. (11).

Besides the nZVI, the stabilized iron sulfide FeS nanoparticles also expressed excellence in POPs degradation. It can degrade the lindane herbicide in its hexane extract with an efficiency higher than 94%. The 1,2,4-trichlorobenzene was a main intermediate of the degradation pathway of lindane. Comparatively, the non-stabilized FeS nanoparticles can degrade lindane only 25% which is much lower than the

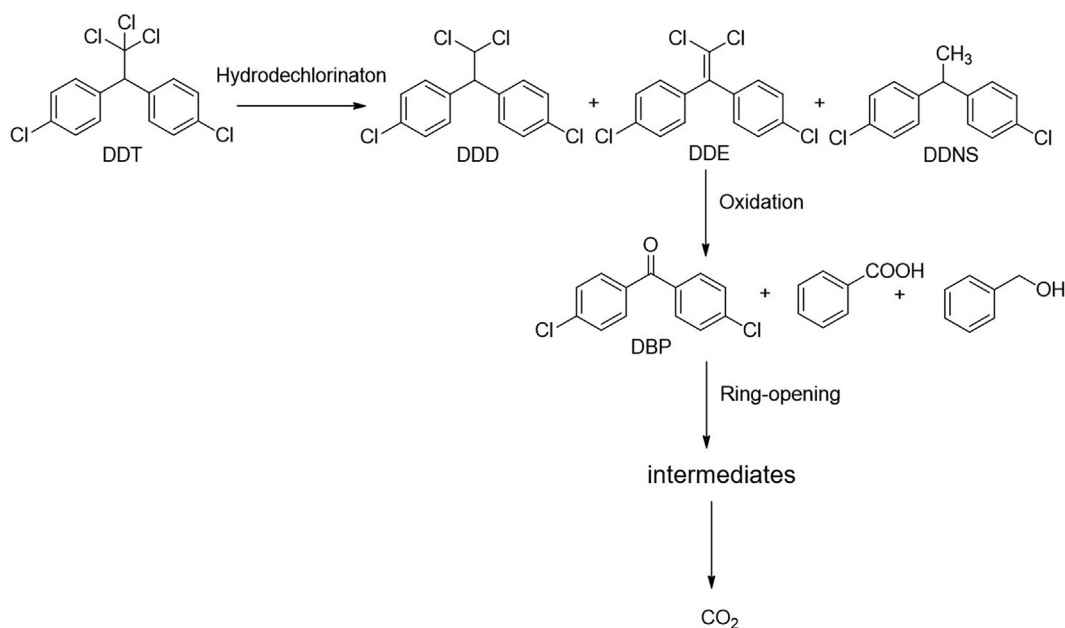


Fig. 6 The intermediates and degradation pathway for DDT using persulfate activation by nZVI.

efficiency obtained from the stabilized FeS. It is obviously indicated that these FeS nanoparticles rapidly catalyzed a reductive dehalogenation reaction (Assaf-Anid and Kun-Yu, 2002; Paknikar et al., 2005). In addition, effective DDT abatement can be achieved by using persulfate activation by nZVI with the proposed degradation pathway described as shown in Fig. 6 (Zhu et al., 2016).

5. Removal of POP using other photocatalysts

As previously described, metal oxide based materials, especially TiO₂, are dominated photocatalysts for the degradation of water pollutants. This section aims to cover comprehensive details of less conventional photocatalysts involved in POP degradation. UV light responsive nanostructured ZnS catalysts were employed in the reductive dehalogenation of hexafluorobenzene (Yin et al., 2001) and of 2,2',4,4',5,5'-hexachlorobiphenyl (He et al., 2013). Notably, CdS is an efficient photocatalyst in reductive dechlorination of hexachlorobenzene under visible light irradiation after 6 h treatment (Yin et al., 2001).

Limited numbers of polyoxometalates (POMs) were reported as photocatalysts in the degradation of POPs, including polyoxotungstates (Antonaraki et al., 2010), heteropolyoxoanions [SiW₁₂O₄₀]⁴⁻ and [PW₁₂O₄₀]⁴⁻ (Youssef et al., 2019), and amine-functionalized mesoporous silica impregnated with transition-metal-monosubstituted POMs (Li et al., 2006). Bearing metal oxide polyanionic clusters, POMs are generally applied in both acid and redox catalytic processes. It was reported that, [SiW₁₂O₄₀]⁴⁻ was a superior photocatalyst in the degradation of dieldrin, a highly toxic insecticide, under UV light irradiation in comparison to [PW₁₂O₄₀]⁴⁻ (Youssef et al., 2019). Comparable photocatalytic activity of amine-modified MCM-48 attached with K₅[M(H₂O)PW₁₁O₃₉], where M = Co or Ni in the dechlorination of hexachlorobenzene under UV light irradiation was

reported by Li and coworkers (Li et al., 2006). Note that, in the presence of H₃PW₁₂O₄₀, catalytic degradation of lindane (hexachlorocyclohexane) under UV-Vis light irradiation, resulted in chlorobenzenes and chlorophenol byproducts, similar to that found in POMs/TiO₂ photocatalytic systems (Antonaraki et al., 2010; Chen et al., 2004).

Furthermore, Chen and coworker (Chen et al., 2018) reported utilizing graphite oxide/Ag₃PO₄ as a heterojunction photocatalyst accelerated debromination of decabromodiphenyl ether diluted in tetrahydrofuran and water under visible light irradiation and N₂ atmosphere. The graphite oxide 2D material acts as protective sheets for Ag₃PO₄ particles, promoting electron-hole pair separation and electron transfer at the graphite oxide and Ag₃PO₄ interface to accelerate decabromodiphenyl ether degradation. Notably, graphite oxide/Ag₃PO₄ composite shows a much lower photocatalytic activity (*ca.* 10 folds) at a slower rate in the debromination of decabromodiphenyl ether soluble in tetrahydrofuran/methanol mixture, compared with that of g-C₃N₄/Fe₂O₃ system, in which the electron hole pair recombination was suppressed by g-C₃N₄ nanosheets (Shao et al., 2018).

Porous materials have advantages as catalysts generally containing a large number of active sites on both the external and internal surfaces of the materials. MOFs (Wang et al., 2020), coordination complexes of metal ions or cluster and organic ligands, are classified as a porous crystalline solids generally having a high surface area. The pore structure and energy bandgap of MOFs are tunable depending on the selections of metal ion clusters and organic linkers (Choi et al., 2009; Lin et al., 2012; Pham et al., 2014). Consequently, high specific surface area MOFs with varied bandgap energy are extensively applied as catalysts in controlled photochemical organic synthesis (Pascanu et al., 2019), and the remediation of versatile toxic, non-biodegradable water pollutants *e.g.* dyes, pesticides, pharmaceuticals and personal care product related pollutants (Pi et al., 2018; Wang et al., 2020). Nevertheless, a very small number of MOFs were reported as efficient

photocatalysts in the degradation of POPs (Stockholm's list) and their derivatives. The dechlorination of 1,1-bis(4-chlorophenyl)-2,2,2-trichloroethane under visible light irradiation catalyzed by B₁₂-Ru@MOF for 4 h resulted in 99% and 63% yields of or DDT to 1,1-bis(4-chlorophenyl)-2,2-dichloroethane in the 1st and 3rd cycles, respectively. The reactions were performed under N₂ atmosphere with the addition of triethanolamine hole scavenger (Xu et al., 2015). Some recent work (Peng et al., 2020) reported on the utilization of ammine functionalized MIL-125(Ti) as a visible light responsive catalyst in the reductive debromination of decabromodiphenyl ether with triethanolamine addition. With added scavengers, the debromination of decabromodiphenyl ether was achievable via the pathway involved electrons stored on the conduction band (or lowest unoccupied molecular orbitals) in MOFs.

In the past few decades, metal-free photocatalysts have attracted a great attention due to their unique characteristics i.e. tunable structures, excellent stability, favorable thermal and electrical conductivity, strong interactions with substrates, and abundant supply for potential large-scale applications (Nikokavoura and Trapalis, 2017). Graphitic carbon nitride (g-C₃N₄), obtained from the thermal polycondensation of dicyandiamide, was reported as a UV responsive catalyst in the debromination of decabrominated diphenyl ethers in methanol, resulting in the formation of hexa- and pentabrominated byproducts after 8 h (Sun et al., 2012).

In addition, polymeric photosensitizers and antenna polyelectrolytes are photocatalysts applicable in the detoxification of POPs, and several non-biodegradable water pollutants (Nowakowska and Szczubiańska, 2017). The polymers are photoresponsive, absorb light to induce photochemical reactions, as they may contain aromatic chromophore covalently attached on the polymeric chains, adsorbed or encapsulated in the polymer matrix. Additionally, they are amphiphilic, thus assist in the solubilization of poorly water-soluble organic compounds through the formation of micelle like complexes (Nowakowska and Guillet, 1991; Sustar et al., 1992). Carbazole (Nowakowska and Szczubiańska, 1999) and naphthalene (Nowakowska et al., 1991; Sustar et al., 1992) functionalized polymers were used in detoxification of polluted water containing hexachlorobenzene and polychlorinated, respectively. Solubilization and photosensitized dechlorination of the polychlorinated pollutants resulted in the formation of degradation products with less chlorinated congeners.

Moreover, recently developed metal-free photocatalysts for environmental applications are microporous organic polymers (MOPs), also known as polymers of intrinsic microporosity, covalent organic framework, hypercrosslinked polymers, and conjugated microporous polymers. One of the advantages of MOPs over inorganic semiconductors that has been pronounced is that their optical and electronic properties are tunable by varying aromatic building blocks with a range of functional groups (Lan et al., 2018; Wang et al., 2018). The average pore dimension, volume, pore size distribution, and specific surface area of MOPs also can be finely tuned by controlled polymerization processes (Xiao et al., 2019). Although, up to now, the photocatalyst activity of MOPs was reported as being efficient in the degradation of several organic dyes (Tang et al., 2019; Xiao et al., 2019) and chemical warfare agents (Ma et al., 2019), these materials could have a high potentials in highly persistent water pollutants including POPs.

6. Concluding remarks and perspectives

In this review, we have collected and highlighted a series of potential photocatalysts, such as TiO₂-based, ZnS, CdS, POMs, MOFs, MOPs, polymeric photosensitizers, etc., with the high-performance to eliminate POPs completely. Among candidates, TiO₂-based photocatalysts for POP photocatalytic removal have attracted considerable interest. In addition, various technologies, reaction conditions, mechanisms, and kinetics for the photocatalytic degradation of POPs have been profitably proposed and discussed by many groups:

1. **TiO₂-based photocatalysts:** to immobilize semiconductor photocatalysts on different supports could neglect the numerous disadvantages correlated with the suspension system (such as recovering the suspended TiO₂ powders from the effluent stream, ready for sizeable scale-up photoreactor, etc.). However, it has been suggested to improve photocatalyst coating layers to achieve more homogeneity and crystallinity by exploring new methods/techniques. Additionally, another approach is doping with the metal/nonmetal nanoparticles, coupling with the semiconductor materials, or hybridizing with the addition of oxidants for widening into the visible light absorption are also proposed.
2. **Other types of photocatalysts:** many photocatalyst systems have been successfully evaluated for the photocatalytic removal of POPs, such as ZnS, CdS, POMs, MOFs, MOPs, polymeric photosensitizers, etc. These candidates also show a high potential in photo-removal of POPs in the future.
3. **Reaction conditions:** to optimize the reaction parameters and reactor configurations for typical types of POPs, such as catalyst dosage, light sources (wavelength, intensity, light distribution, and utilization, etc.), POPs properties and its feed ratio, etc.
4. **Fenton reactions:** In addition to photocatalysis, Fenton, Fenton-like, and photo-Fenton reactions have been studied to evaluate the removal performance of POPs. The idea final products of these reactions are CO₂ and water, which are friendly to the environment. The disadvantages of this concept are the reactions require to be set up at acid conditions (pH = 2–4), and the generated iron sludge after the reaction.

To further improve the photocatalytic performance, some critical points could be considered as follows:

1. **Photocatalysts:** to simplify the current synthesis methods, and to continue improving light-harvesting, promoting charge carrier separation, inhibiting the recombination of electrons and holes, offering more active sites, etc.
2. **Mechanisms, reaction pathways:** to disclose and figure out the photocatalytic mechanisms, reaction pathways, kinetics for the photocatalytic removal of POPs from molecular insights to large-scale applications.
3. **Photo-reactors:** to design and propose a new reactor system with optimizing operation parameters which have considered many factors, including mass transfer; photon transfer, distribution, and utilization, etc. Importantly, it should be ready and available for large-scale applications.

Declaration of Competing Interest

The authors declared that there is no conflict of interest.

Acknowledgment

This work was partially supported by Thailand Research Fund (Grant No. BRG6180009 and Grant No. IRN62W0005) for Puangrat Kajitvichyanukul and Siwaporn Meejoo Smith. This research work was partially supported by Chiang Mai University, Thailand.

References

- Abdelhaleem, A., Chu, W., 2020. Prediction of carbofuran degradation based on the hydroxyl radical's generation using the Fe^{III} impregnated N doped-TiO₂/H₂O₂/visible LED photo-Fenton-like process. *Chem. Eng. J.* 382, <https://doi.org/10.1016/j.cej.2019.122930> 122930.
- Al-Mulali, U., Ozturk, I., Lean, H.H., 2015. The influence of economic growth, urbanization, trade openness, financial development, and renewable energy on pollution in Europe. *Nat. Hazards*. 79 (1), 621–644. <https://doi.org/10.1007/s11069-015-1865-9>.
- Ananpattarachai, J., Kajitvichyanukul, P., 2015. Photocatalytic degradation of p, p'-DDT under UV and visible light using interstitial N-doped TiO₂. *J. Environ. Sci. Health - Part B*. 50 (4), 247–260. <https://doi.org/10.1080/03601234.2015.999592>.
- Ananpattarachai, J., Kajitvichyanukul, P., Seraphin, S., 2009. Visible light absorption ability and photocatalytic oxidation activity of various interstitial N-doped TiO₂ prepared from different nitrogen dopants. *J. Hazard. Mater.* 168 (1), 253–261. <https://doi.org/10.1016/j.jhazmat.2009.02.036>.
- Ananpattarachai, J., Boonto, Y., Kajitvichyanukul, P., 2016a. Visible light photocatalytic antibacterial activity of Ni-doped and N-doped TiO₂ on *Staphylococcus aureus* and *Escherichia coli* bacteria. *Environ. Sci. Pollut. Res.* 23 (5), 4111–4119. <https://doi.org/10.1007/s11356-015-4775-1>.
- Ananpattarachai, J., Seraphin, S., Kajitvichyanukul, P., 2016b. Formation of hydroxyl radicals and kinetic study of 2-chlorophenol photocatalytic oxidation using C-doped TiO₂, N-doped TiO₂, and C, N Co-doped TiO₂ under visible light. *Environ. Sci. Pollut. Res.* 23 (4), 3884–3896. <https://doi.org/10.1007/s11356-015-5570-8>.
- Andersen, J., Pelaez, M., Guay, L., Zhang, Z., O'Shea, K., Dionysiou, D.D., 2013. NF-TiO₂ photocatalysis of amitrole and atrazine with addition of oxidants under simulated solar light: Emerging synergies, degradation intermediates, and reusable attributes. *J. Hazard. Mater.* 260, 569–575. <https://doi.org/10.1016/j.jhazmat.2013.05.056>.
- Antonarakis, S., Triantis, T., Papaconstantinou, E., Hiskia, A., 2010. Photocatalytic degradation of lindane by polyoxometalates: intermediates and mechanistic aspects. *Catal. Today*. 151 (1–2), 119–124. <https://doi.org/10.1016/j.cattod.2010.02.017>.
- Antonopoulou, M., Vlastos, D., Konstantinou, I., 2015. Photocatalytic degradation of pentachlorophenol by N-F-TiO₂: identification of intermediates, mechanism involved, genotoxicity and ecotoxicity evaluation. *Photochem. Photobiol. Sci.* 14 (3), 520–527. <https://doi.org/10.1039/C4PP00254G>.
- Ashraf, M.A., 2017. Persistent organic pollutants (POPs): a global issue, a global challenge. *Environ. Sci. Pollut. Res.* 24 (5), 4223–4227. <https://doi.org/10.1007/s11356-015-5225-9>.
- Assaf-Anid, N., Lin, K.Y., 2002. Carbon tetrachloride reduction by Fe²⁺, S²⁻, and FeS with vitamin B12 as organic amendment. *J. Environ. Eng.* 128 (1), 94–99. [https://doi.org/10.1061/\(asce\)0733-9372\(2002\)128:1\(94\)](https://doi.org/10.1061/(asce)0733-9372(2002)128:1(94)).
- Agency for Toxic Substances and Disease Registry- US Public Health Service, 1995. Toxicological Profile for Mirex and Chlordecone, Atlanta.
- Agency for Toxic Substances and Disease Registry-US Public Health Service, 2004. Toxicological Profile for Polybrominated Biphenyls and Polybrominated Diphenyl Ethers. Dept Health and Human Services Agency for Toxic Substances and Disease Registry. Atlanta, pp. 357
- Agency for Toxic Substances and Disease Registry- US Public Health Service, 2015. Toxicological Profile for Perfluoralkyls. Atlanta.
- Avetta, P., Pensato, A., Minella, M., Malandrino, M., Maurino, V., Minero, C., Hanna, K., Vione, D., 2015. Activation of persulfate by irradiated magnetite: Implications for the degradation of phenol under heterogeneous photo-Fenton-like conditions. *Environ. Sci. Technol.* 49, 1043–1050. <https://doi.org/10.1021/es503741d>.
- Aziz, H. A., Alias, S., Adlan, M. N., Faridah, Asaari, A. H., Zahari, M. S., 2007. Colour removal from landfill leachate by coagulation and flocculation processes. *Bioresour. Technol.* 98(1), 218–220. <https://doi.org/10.1016/j.biortech.2005.11.013>
- Bailey, R.E., Wijk, D.V., Thomas, C.P., 2009. Sources and prevalence of pentachlorobenzene in the environment. *Chemosphere* 75 (5), 555–564. <https://doi.org/10.1016/j.chemosphere.2009.01.038>.
- Bakirtas, T., Akpolat, A.G., 2018. The relationship between energy consumption, urbanization, and economic growth in new emerging-market countries. *Energy*. 147, 110–121. <https://doi.org/10.1016/j.energy.2018.01.011>.
- Balaşubramanian, G., Dionysiou, D. D., Suidan, M. T., Baudin, I., Laine, J.-M., 2004. Evaluating the activities of immobilized TiO₂ powder films for the photocatalytic degradation of organic contaminants in water. *Appl. Catal., B-Environ.* 47(2), 73–84. <https://doi.org/10.1016/j.apcatb.2003.04.002>.
- Bastos, P.M., Eriksson, J., Vidarson, J., Bergman, Å., 2008. Oxidative transformation of polybrominated diphenyl ether congeners (PBDEs) and of hydroxylated PBDEs (OH-PBDEs). *Environ. Sci. Pollut. Res. Int.* 15 (7), 606–613. <https://doi.org/10.1007/s11356-008-0045-9>.
- Bastos, P.M., Eriksson, J., Bergman, Å., 2009. Photochemical decomposition of dissolved hydroxylated polybrominated diphenyl ethers under various aqueous conditions. *Chemosphere* 77 (6), 791–797. <https://doi.org/10.1016/j.chemosphere.2009.08.013>.
- Borba, F.H., Pellenz, L., Bueno, F., Inticher, J.J., Braun, L., Espinoza-Quiñones, F.R., Trigueros, D.E.G., De Pauli, A.R., Módenes, A.N., 2018. Pollutant removal and biodegradation assessment of tannery effluent treated by conventional Fenton oxidation process. *J. Environ. Chem. Eng.* 6, 7070–7079. <https://doi.org/10.1016/j.jece.2018.11.005>.
- Bu, Q., Shi, X., Yu, G., Huang, J., Wang, B., 2016. Assessing the persistence of pharmaceuticals in the aquatic environment: Challenges and needs. *Emerg. Contam.* 2 (3), 145–147. <https://doi.org/10.1016/j.emcon.2016.05.003>.
- Budavari, S. (Ed.), 1996. The Merck Index - An encyclopedia of chemicals, drugs, and biologicals. Whitehouse Station, NJ Merck Co. New Jersey.
- Byrappa, K., Lokanatha Rai, K.M., Yoshimura, M., 2000. Hydrothermal preparation of TiO₂ and photocatalytic degradation of hexachlorocyclohexane and dichlorodiphenyltrichloromethane. *Environ. Tech.* 21 (10), 1085–1090. <https://doi.org/10.1080/09593330.2000.9618994>.
- Canadian Environmental Protection Act, 1999. Environmental Screening Assessment Report on Polybrominated Diphenyl Ethers (PBDEs).
- Chen, C., Lei, P., Ji, H., Ma, W., Zhao, J., Hidaka, H., Serpone, N., 2004. Photocatalysis by titanium dioxide and polyoxometalate/TiO₂ cocatalysts. Intermediates and mechanistic study. *Environ. Sci. Technol.* 38 (1), 329–337. <https://doi.org/10.1021/es034384f>.
- Chen, M.-J., Lo, S.-L., Lee, Y.-C., Kuo, J., Wu, C.-H., 2016. Decomposition of perfluorooctanoic acid by ultraviolet light

- irradiation with Pb-modified titanium dioxide. *J. Hazard. Mater.* 303, 111–118. <https://doi.org/10.1016/j.jhazmat.2015.10.011>.
- Chen, W., Niu, X., Wang, J., 2018. A photocatalyst of graphene oxide (GO)/Ag₃PO₄ with excellent photocatalytic activity over decabromodiphenyl ether (BDE-209) under visible light irradiation. *J. Photochem. Photobiol.* 356, 304–311. <https://doi.org/10.1016/j.jphotochem.2017.12.038>.
- Chen, X., Shen, S., Guo, L., Mao, S.S., 2010. Semiconductor-based Photocatalytic Hydrogen Generation. *Chem. Rev.* 110 (11), 6503–6570. <https://doi.org/10.1021/cr1001645>.
- Choi, J.H., Choi, Y.J., Lee, J.W., Shin, W.H., Kang, J.K., 2009. Tunability of electronic band gaps from semiconducting to metallic states via tailoring Zn ions in MOFs with Co ions. *Phys. Chem. Chem. Phys.* 11 (4), 628–631. <https://doi.org/10.1039/B816668D>.
- Choi, W., Hoffmann, M.R., 1995. Photoreductive mechanism of CCl₄ degradation on TiO₂ particles and effects of electron donors. *Environ. Sci. Technol.* 29 (6), 1646–1654. <https://doi.org/10.1021/es00006a031>.
- Choi, W., Termin, A., Hoffmann, M.R., 1994. The role of metal ion dopants in quantum-sized TiO₂: correlation between photoreactivity and charge carrier recombination dynamics. *J. Phys. Chem.* 98 (51), 13669–13679. <https://doi.org/10.1021/j100102a038>.
- Choi, W., Hong, S.J., Chang, Y.S., Cho, Y., 2000. Photocatalytic degradation of polychlorinated dibenzo-p-dioxins on TiO₂ film under UV or solar light irradiation. *Environ. Sci. Technol.* 34 (22), 4810–4815. <https://doi.org/10.1021/es0011461>.
- Chong, M.N., Jin, B., Chow, C.W.K., Saint, C., 2010. Recent developments in photocatalytic water treatment technology: A review. *Water Res.* 44 (10), 2997–3027. <https://doi.org/10.1016/j.watres.2010.02.039>.
- Clara, M., Strenn, B., Gans, O., Martinez, E., Kreuzinger, N., Kroiss, H., 2005. Removal of selected pharmaceuticals, fragrances and endocrine disrupting compounds in a membrane bioreactor and conventional wastewater treatment plants. *Water Res.* 39, 4797–4807. <https://doi.org/10.1016/j.watres.2005.09.015>.
- Correia de Velosa, A., Pupo Nogueira, R.F., 2013. 2,4-Dichlorophenoxyacetic acid (2,4-D) degradation promoted by nanoparticulate zerovalent iron (nZVI) in aerobic suspensions. *J. Environ. Manage.* 121, 72–79. <https://doi.org/10.1016/j.jenvman.2013.02.031>.
- Davididou, K., Chatzisyemon, E., Perez-Estrada, L., Oller, I., Malato, S., 2019. Photo-Fenton treatment of saccharin in a solar pilot compound parabolic collector: Use of olive mill wastewater as iron chelating agent, preliminary results. *J. Hazard. Mater.* 372, 137–144. <https://doi.org/10.1016/j.jhazmat.2018.03.016>.
- De Bruijn, J., Hermens, J., 1991. Uptake and elimination kinetics of organophosphorous pesticides in the guppy (*Poecilia reticulata*): Correlations with the octanol/water partition coefficient. *Environ. Toxicol. Chem.* 10 (6), 791–804. <https://doi.org/10.1002/etc.5620100610>.
- Deng, J., Shao, Y., Gao, N., Deng, Y., Tan, C., Zhou, S., 2014. Zero-valent iron/persulfate(Fe⁰/PS) oxidation acetaminophen in water. *Int. J. Environ. Sci. Technol.* 11, 881–890. <https://doi.org/10.1007/s13762-013-0284-2>.
- Dillert, R., Bahnemann, D., Hidaka, H., 2007. Light-induced degradation of perfluorocarboxylic acids in the presence of titanium dioxide. *Chemosphere* 67 (4), 785–792. <https://doi.org/10.1016/j.chemosphere.2006.10.023>.
- Do, H.-T., Phan Thi, L.-A., Dao Nguyen, N.H., Huang, C.-W., Le, Q.V., Nguyen, V.-H., 2020. Tailoring photocatalysts and elucidating mechanisms of photocatalytic degradation of perfluorocarboxylic acids (PFCAs) in water: a comparative overview. *J. Chem. Technol. Biotechnol.* <https://doi.org/10.1002/jctb.6333>.
- Doll, T.E., Frimmel, F.H., 2003. Fate of pharmaceuticals—photodegradation by simulated solar UV-light. *Chemosphere* 52 (10), 1757–1769. [https://doi.org/10.1016/S0045-6535\(03\)00446-6](https://doi.org/10.1016/S0045-6535(03)00446-6).
- Dong, H., Zeng, G., Tang, L., Fan, C., Zhang, C., He, X., He, Y., 2015. An overview on limitations of TiO₂-based particles for photocatalytic degradation of organic pollutants and the corresponding countermeasures. *Water Res.* 79, 128–146. <https://doi.org/10.1016/j.watres.2015.04.038>.
- European Chemical Agency: Risk assessment of hexabromocyclododecane, 2008. <https://echa.europa.eu/documents/10162/661bff17-dc0a-4475-9758-40bdd6198f82> (accessed 18 April 2020).
- El-Shahawi, M.S., Hamza, A., Bashammakh, A.S., Al-Saggaf, W.T., 2010. An overview on the accumulation, distribution, transformations, toxicity and analytical methods for the monitoring of persistent organic pollutants. *Talanta* 80 (5), 1587–1597. <https://doi.org/10.1016/j.talanta.2009.09.055>.
- Eriksson, J., Green, N., Marsh, G., Bergman, Å., 2004. Photochemical decomposition of 15 polybrominated diphenyl ether congeners in methanol/water. *Environ. Sci. Technol.* 38 (11), 3119–3125. <https://doi.org/10.1021/es049830t>.
- Esaac, E.G., Matsumura, F., 1980. Metabolism of insecticides by reductive systems. *Pharmacol. Ther.* 9 (1), 1–26. [https://doi.org/10.1016/0163-7258\(80\)90014-5](https://doi.org/10.1016/0163-7258(80)90014-5).
- Office for Official Publications of the European Committees-European Union, 2001. Diphenyl ether, pentabromo derivative (pentabromodiphenyl ether). Luxembourg, European Union Risk Assessment Report, pp. 1-124.
- Friesen, K.J., Foga, M.M., Loewen, M.D., 1996. Aquatic photodegradation of polychlorinated dibenzofurans: rates and photoproduct analysis. *Environ. Sci. Technol.* 30, 2504–2510. <https://doi.org/10.1021/es9508277>.
- Fu, J., Kyzas, G.Z., Cai, Z., Deliyanni, E.A., Liu, W., Zhao, D., 2018. Photocatalytic degradation of phenanthrene by graphite oxide-TiO₂-Sr(OH)₂/SrCO₃ nanocomposite under solar irradiation: Effects of water quality parameters and predictive modeling. *Chem. Eng. J.* 335, 290–300. <https://doi.org/10.1016/j.cej.2017.10.163>.
- Fu, Y.-S., Li, J., Li, J., 2019. Metal/Semiconductor Nanocomposites for Photocatalysis: Fundamentals, Structures Applications and Properties. *Nanomaterials* 9 (3), 359. <https://doi.org/10.3390/nano9030359>.
- Garcia-Segura, S., Anotai, J., Singhadech, S., Lu, M.C., 2017. Enhancement of biodegradability of o-toluidine effluents by electro-assisted photo-Fenton treatment. *Process Saf. Environ. Prot.* 106, 60–67. <https://doi.org/10.1016/j.psep.2016.12.011>.
- Gomez-Ruiz, B., Ribao, P., Diban, N., Rivero, M.J., Ortiz, I., Urtiaga, A., 2018. Photocatalytic degradation and mineralization of perfluorooctanoic acid (PFOA) using a composite TiO₂-rGO catalyst. *J. Hazard. Mater.* 344, 950–957. <https://doi.org/10.1016/j.jhazmat.2017.11.048>.
- Govindan, K., Murugesan, S., Maruthamuthu, P., 2013. Photocatalytic degradation of pentachlorophenol in aqueous solution by visible light sensitive NF-codoped TiO₂ photocatalyst. *Mater. Res. Bull.* 48 (5), 1913–1919. <https://doi.org/10.1016/j.materresbull.2013.01.047>.
- Graça, C.A.L., Fugita, L.T.N., de Velosa, A.C., Teixeira, A.C.S.C., 2018. Amicarbazone degradation promoted by ZVI-activated persulfate: study of relevant variables for practical application. *Environ. Sci. Pollut. Res.* 25, 5474–5483. <https://doi.org/10.1007/s1356-017-0862-9>.
- Guo, L., Zhang, K., Han, X., Zhao, Q., Wang, D., Fu, F., Liang, Y., 2020. Highly efficient visible-light-driven photo-Fenton catalytic performance over FeOOH/Bi₂WO₆ composite for organic pollutant degradation. *J. Alloys Compd.* 816. <https://doi.org/10.1016/j.jallcom.2019.152560> 152560.
- Hagenmaier, H., She, J., Lindig, C., 1992. Proceedings of the Eleventh International Symposium Persistence of polychlorinated dibenzo-p-dioxins and polychlorinated dibenzofurans in contaminated soil at Maulach and Rastatt in Southwest Germany. *Chemosphere* 25 (7), 1449–1456.
- Hansch, C., A. Leo., 1979. Substituent Constants for Correlation Analysis in Chemistry and Biology. John Wiley and Sons, New York.
- Hansch, C., Leo, A., Hoekman, D., 1995. Exploring QSAR. Hydrophobic, electronic, and steric constants. ACS Professional

- Reference Book. ACS, Washington. <https://doi.org/10.1021/jm950902o>.
- Hansen, K.J., Clemen, L.A., Ellefson, M.E., Johnson, H.O., 2001. Compound-specific, quantitative characterization of organic fluorochemicals in biological matrices. *Environ. Sci. Technol.* 35 (4), 766–770. <https://doi.org/10.1021/es001489z>.
- Hardy, M.L., 2002. A comparison of the properties of the major commercial PBDPO/PBDE product to those of major PBB and PCB products. *Chemosphere* 46 (5), 717–728. [https://doi.org/10.1016/S0045-6535\(01\)00236-3](https://doi.org/10.1016/S0045-6535(01)00236-3).
- Hartley, D. and H. Kidd (Eds.), 1983. *The Agrochemicals Handbook*. Surrey, Royal Society of Chemistry.
- Haynes, W.M. (Ed.) 2010, *CRC Handbook of Chemistry and Physics*. 91st edition. Boca Raton, CRC Press Inc., pp. 3-420
- He, L., Xiong, Y., Zhao, M., Mao, X., Liu, Y., Zhao, H., Tang, Z., 2013. Bioinspired Synthesis of ZnS supraparticles toward photoinduced dechlorination of 2, 2', 4, 4', 5, 5'-Hexachlorobiphenyl. *Chem. Asian J.* 8 (8), 1765–1767. <https://doi.org/10.1002/asia.201300277>.
- Hewer, T.L.R., Suárez, S., Coronado, J.M., Portela, R., Avila, P., Sanchez, B., 2009. Hybrid photocatalysts for the degradation of trichloroethylene in air. *Catal. Today*. 143 (3), 302–308. <https://doi.org/10.1016/j.cattod.2009.02.001>.
- Hu, Y., Li, D., Zheng, Y., Chen, W., He, Y., Shao, Y., Fu, X., Xiao, G., 2011. BiVO₄/TiO₂ nanocrystalline heterostructure: A wide spectrum responsive photocatalyst towards the highly efficient decomposition of gaseous benzene. *Appl. Catal. B-Environ.* 104 (1), 30–36. <https://doi.org/10.1016/j.apcatb.2011.02.031>.
- International Agency For Research on Cancer Polychlorinated and Polybrominated Biphenyls Volume 18, 1978, Lyon.
- International Agency for Research on Cancer Monographs, 1979. Evaluation of the Carcinogenic Risk of Chemicals to Man. Geneva, Switzerland: WHO International Agency for Research on Cancer. 20, 180, Lyon.
- International Agency for Research on Cancer Monographs, 1999. Evaluation of the Carcinogenic Risk of Chemicals to Humans. 71, 1365, Lyon.
- Ide, A., Niki, Y., Sakamoto, F., Watanabe, I., 1972. Decomposition of pentachlorophenol in paddy soil. *Agric Biol Chem.* 36, 1937–1944. <https://doi.org/10.1080/00021369.1972.10860498>.
- Jing, C., Pengyi, Z., Li, Z., 2006. Photocatalytic decomposition of environmentally persistent perfluorooctanoic acid. *Chem. Lett.* 35 (2), 230–231. <https://doi.org/10.1246/cl.2006.230>.
- Jones, K.C., de Voogt, P., 1999. Persistent organic pollutants (POPs): state of the Science. *Environ. Pollut.* 100 (1), 209–221. [https://doi.org/10.1016/S0269-7491\(99\)00098-6](https://doi.org/10.1016/S0269-7491(99)00098-6).
- Kahoush, M., Behary, N., Cayla, A., Nierstrasz, V., 2018. Bio-Fenton and Bio-electro-Fenton as sustainable methods for degrading organic pollutants in wastewater. *Process Biochem.* 64, 237–247. <https://doi.org/10.1016/j.procbio.2017.10.003>.
- Katsoyiannis, A., Samara, C., 2004. Persistent organic pollutants (POPs) in the sewage treatment plant of Thessaloniki, northern Greece: occurrence and removal. *Water Res* 38 (11), 2685–2698. <https://doi.org/10.1016/j.watres.2004.03.027>.
- Katsoyiannis, A., Samara, C., 2005. Persistent organic pollutants (POPs) in the conventional activated sludge treatment process: Fate and mass balance. *Environ. Res.* 97, 245–257. <https://doi.org/10.1016/j.envres.2004.09.001>.
- Katsumata, H., Kaneco, S., Suzuki, T., Ohta, K., Yobiko, Y., 2006. Degradation of polychlorinated dibenzo-p-dioxins in aqueous solution by Fe(II)/H₂O₂/UV system. *Chemosphere* 63 (4), 592–599. <https://doi.org/10.1016/j.chemosphere.2005.08.015>.
- UV and sunlight, in: Agnihotri, A., Reddy, K., Bansal A. (Eds), *Sustainable Engineering. Lecture Notes in Civil Engineering*, vol 30. Springer, Singapore, pp.145-155. 10.1007/978-981-13-6717-5_15
- Khan, J.A., Han, C., Shah, N.S., Khan, H.M., Nadagouda, M.N., Likodimos, V., Falaras, P., O'Shea, K., Dionysiou, D.D., 2014. Ultraviolet-Visible light-sensitive high surface area phosphorous-fluorine-co-doped TiO₂ nanoparticles for the degradation of atrazine in water. *Environ. Eng. Sci.* 31 (7), 435–446. <https://doi.org/10.1089/ees.2013.0486>.
- Kim, M., O'keefe, P. W., 2000. Photodegradation of polychlorinated dibenzo-p-dioxins and dibenzofurans in aqueous solutions and in organic solvents. *Chemosphere*. 41(6), 793-800. 10.1016/S0045-6535(99)00564-0
- Kozhevnikova, N.S., Gorbunova, T.I., Vorokh, A.S., Pervova, M.G., Zapevalov, A.Y., Saloutin, V.I., Chupakhin, O.N., 2019. Nanocrystalline TiO₂ doped by small amount of pre-synthesized colloidal CdS nanoparticles for photocatalytic degradation of 1,2,4-trichlorobenzene. *Sustain. Chem. Pharm.* 11, 1–11. <https://doi.org/10.1016/j.scp.2018.11.004>.
- Lan, Z.A., Fang, Y., Zhang, Y., Wang, X., 2018. Photocatalytic oxygen evolution from functional triazine-based polymers with tunable band structures. *Angew. Chem. Int. Ed.* 57 (2), 470–474. <https://doi.org/10.1002/anie.201711155>.
- Le Cunff, J., Tomašić, V., Wittine, O., 2015. Photocatalytic degradation of the herbicide terbuthylazine: Preparation, characterization and photoactivity of the immobilized thin layer of TiO₂/chitosan. *J. Photochem. Photobiol.* 309, 22–29. <https://doi.org/10.1016/j.jphotochem.2015.04.021>.
- Leong, K.H., Benjamin Tan, L.L., Mustafa, A.M., 2007. Contamination levels of selected organochlorine and organophosphate pesticides in the Selangor River, Malaysia between 2002 and 2003. *Chemosphere* 66 (6), 1153–1159. <https://doi.org/10.1016/j.chemosphere.2006.06.009>.
- Li, T., Li, X., Zhao, Q., Shi, Y., Teng, W., 2014. Fabrication of n-type CuInS₂ modified TiO₂ nanotube arrays heterostructure photoelectrode with enhanced photoelectrocatalytic properties. *Appl. Catal B-Environ.* 156–157, 362–370. <https://doi.org/10.1016/j.apcatb.2014.03.035>.
- Li, L., Liu, C., Geng, A., Jiang, C., Guo, Y., Hu, C., 2006. Preparation, characterization and photocatalytic applications of amine-functionalized mesoporous silica impregnated with transition-metal-monosubstituted polyoxometalates. *Mater. Res. Bull.* 41 (2), 319–332. <https://doi.org/10.1016/j.materresbull.2005.08.013>.
- Li, H., Wan, J., Ma, Y., Wang, Y., Guan, Z., 2015. Role of inorganic ions and dissolved natural organic matters on persulfate oxidation of acid orange 7 with zero-valent iron. *RSC Adv.* 5, 99935–99943. <https://doi.org/10.1039/c5ra16094d>.
- Li, K., Xiong, J., Chen, T., Yan, L., Dai, Y., Song, D., Lv, Y., Zeng, Z., 2013. Preparation of graphene/TiO₂ composites by nonionic surfactant strategy and their simulated sunlight and visible light photocatalytic activity towards representative aqueous POPs degradation. *J. Hazard. Mater.* 250–251, 19–28. <https://doi.org/10.1016/j.jhazmat.2013.01.069>.
- Li, M., Yu, Z., Liu, Q., Sun, L., Huang, W., 2016. Photocatalytic decomposition of perfluorooctanoic acid by noble metallic nanoparticles modified TiO₂. *Chem. Eng. J.* 286, 232–238. <https://doi.org/10.1016/j.cej.2015.10.037>.
- Lide, D.R., 2000. *CRC Handbook of Chemistry and Physics*. 81st edition. CRC Press, Florida.
- Lin, C., Lin, K.-S., 2007. Photocatalytic oxidation of toxic organohalides with TiO₂/UV: The effects of humic substances and organic mixtures. *Chemosphere* 66 (10), 1872–1877. <https://doi.org/10.1016/j.chemosphere.2006.08.027>.
- Lin, C.-K., Zhao, D., Gao, W.-Y., Yang, Z., Ye, J., Xu, T., Ge, Q., Ma, S., Liu, D.-J., 2012. Tunability of band gaps in metal-organic frameworks. *Inorg. Chem.* 51 (16), 9039–9044. <https://doi.org/10.1021/ic301189m>.
- Linares-Hernández, I., Barrera-Díaz, C., Bilyeu, B., Juárez-García-Rojas, P., Campos-Medina, E., 2010. A combined electrocoagulation-electrooxidation treatment for industrial wastewater. *J. Hazard. Mater.* 175, 688–694. <https://doi.org/10.4028/www.scientific.net/amr.233-235.619>.
- Liu, C., Chen, W., Sheng, Y., Li, L., 2009. Atrazine degradation in solar irradiation/S-doped titanium dioxide treatment. In 2009 3rd

- International Conference on Bioinformatics and Biomedical Engineering, pp. 1-4. IEEE. 10.1109/icbbe.2009.5162423
- Liu, J.W., Han, R., Wang, H.T., Zhao, Y., Chu, Z., Wu, H.Y., 2011. Photoassisted degradation of pentachlorophenol in a simulated soil washing system containing nonionic surfactant Triton X-100 with La-B codoped TiO₂ under visible and solar light irradiation. *Appl. Catal. B-Environ.* 103 (3), 470-478. <https://doi.org/10.1016/j.apcatb.2011.02.013>.
- Liu, B., Li, X., Zhao, Q., Ke, J., Tadé, M., Liu, S., 2016. Preparation of AgInS₂/TiO₂ composites for enhanced photocatalytic degradation of gaseous o-dichlorobenzene under visible light. *Appl. Catal. B-Environ.* 185, 1-10. <https://doi.org/10.1016/j.apcatb.2015.12.003>.
- Liu, Y., Li, Jia, Li, Jiayao, Yan, X., Wang, F., Yang, W., Ng, D.H.L., Yang, J., 2020. Active magnetic Fe³⁺-doped BiOBr micromotors as efficient solar photo-Fenton catalyst. *J. Clean. Prod.* 252. <https://doi.org/10.1016/j.jclepro.2019.119573>
- Llompert, M., Lores, M., Lourido, M., Sánchez-Prado, L., Cela, R., 2003. On-fiber photodegradation after solid-phase microextraction of p'-DDT and two of its major photoproducts, p, p'-DDE and p'-DDD. *J. Chromatogr. A.* 985 (1-2), 175-183. [https://doi.org/10.1016/S0021-9673\(02\)01394-8](https://doi.org/10.1016/S0021-9673(02)01394-8).
- Lopes da Silva, F., Laitinen, T., Pirilä, M., Keiski, R.L., Ojala, S., 2017. Photocatalytic Degradation of Perfluorooctanoic Acid (PFOA) From Wastewaters by TiO₂, In₂O₃ and Ga₂O₃ Catalysts. *Top. Catal.* 60 (17), 1345-1358. <https://doi.org/10.1007/s11244-017-0819-8>.
- Lv, Y., Zhang, Z., Chen, Y., Hu, Y., 2016. A novel three-stage hybrid nano bimetallic reduction/oxidation/biodegradation treatment for remediation of 2,2',4,4'-tetrabromodiphenyl ether. *Chem. Eng. J.* 289, 382-390. <https://doi.org/10.1016/j.cej.2015.12.097>.
- Lyman, W. J., 1985. in: Neely, W.B., Blau, G. E. (Eds.), *Environmental exposure from chemicals*. Vol. 1, Florida, CRC Press, pp. 13-47
- Ma, L., Dong, X., Chen, M., Zhu, L., Wang, C., Yang, F., Dong, Y., 2017. Fabrication and water treatment application of carbon nanotubes (CNTs)-based composite membranes: A review. *Membranes (Basel)*. 7 (1), 1-21. <https://doi.org/10.3390/membranes7010016>.
- Ma, L., Liu, Y., Liu, Y., Jiang, S., Li, P., Hao, Y., Shao, P., Yin, A., Feng, X., Wang, B., 2019. Ferrocene-Linkage-facilitated charge separation in conjugated microporous polymers. *Angew. Chem. Int. Ed* 58 (13), 4221-4226. <https://doi.org/10.1002/anie.201813598>.
- Ma, X.H., Zhao, L., Dong, Y.H., 2020. Oxidation degradation of 2, 2', 5-trichlorodiphenyl in a chelating agent enhanced Fenton reaction: Influencing factors, products, and pathways. *Chemosphere* 125849. <https://doi.org/10.1016/j.chemosphere.2020.125849>.
- MacBean C. (Ed), 2008. e-Pesticide Manual- Hexachlorobenzene (117-84-1). 15th edition, British Crop Protection Council, Alton.
- Mato, Y., Isobe, T., Takada, H., Kanehiro, H., Ohtake, C., Kaminuma, T., 2001. Plastic resin pellets as a transport medium for toxic chemicals in the marine environment. *Environ. Sci. Technol.* 35 (2), 318-324. <https://doi.org/10.1021/es0010498>.
- Megharaj, M., Ramakrishnan, B., Venkateswarlu, K., Sethunathan, N., Naidu, R., 2011. Bioremediation approaches for organic pollutants: A critical perspective. *Environ. Int.* 37 (8), 1362-1375. <https://doi.org/10.1016/j.envint.2011.06.003>.
- Miranda-García, N., Suárez, S., Sánchez, B., Coronado, J.M., Malato, S., Maldonado, M.I., 2011. Photocatalytic degradation of emerging contaminants in municipal wastewater treatment plant effluents using immobilized TiO₂ in a solar pilot plant. *Appl. Catal. B-Environ.* 103 (3), 294-301. <https://doi.org/10.1016/j.apcatb.2011.01.030>.
- Miranda-García, N., Suárez, S., Maldonado, M.I., Malato, S., Sánchez, B., 2014. Regeneration approaches for TiO₂ immobilized photocatalyst used in the elimination of emerging contaminants in water. *Catal. Today*. 230, 27-34. <https://doi.org/10.1016/j.cattod.2013.12.048>.
- Moody, C.A., Field, J.A., 1999. Determination of Perfluorocarboxylates in Groundwater Impacted by Fire-Fighting Activity. *Environ. Sci. Technol.* 33, 2800-2806. <https://doi.org/10.1021/es981355+>.
- Murthy, N.B.K., Kaufman, D.D., Fries, G.F., 1979. Degradation of pentachlorophenol (PCP) in aerobic and anaerobic soil. *J. Environ. Sci. Health B.* 14, 1-14. <https://doi.org/10.1080/03601237909372110>.
- Muto, H., Saitoh, K., Funayama, H., 2001. PCDD/DF formations by the heterogeneous thermal reactions of phenols and their TiO₂ photocatalytic degradation by batch-recycle system. *Chemosphere* 45 (2), 129-136. [https://doi.org/10.1016/S0045-6535\(00\)00552-X](https://doi.org/10.1016/S0045-6535(00)00552-X).
- Navaratna, D., Shu, L., Jegatheesan, V., 2016. Evaluation of herbicide (persistent pollutant) removal mechanisms through hybrid membrane bioreactors. *Bioresour. Technol.* 200, 795-803. <https://doi.org/10.1016/j.biortech.2015.10.041>.
- Nikokavoura, A., Trapalis, C., 2017. Alternative photocatalysts to TiO₂ for the photocatalytic reduction of CO₂. *Appl. Surf. Sci.* 391, 149-174. <https://doi.org/10.1016/j.apsusc.2016.06.172>.
- Nowakowska, M., Guillet, J.E., 1991. Studies of the antenna effect in polymer systems. 18. Photochemical reactions of styrene solubilized in an aqueous solution of poly (sodium styrenesulfonate-co-2-vinylnaphthalene). *Macromolecules* 24 (2), 474-478. <https://doi.org/10.1021/ma00002a021>.
- Nowakowska, M., Szczubiałka, K., 1999. Photosensitized dechlorination of polychlorinated benzenes. 1. Carbazole-photosensitized dechlorination of hexachlorobenzene. *Chemosphere* 39 (1), 71-80. [https://doi.org/10.1016/s0045-6535\(98\)00589-x](https://doi.org/10.1016/s0045-6535(98)00589-x).
- Nowakowska, M., Sustar, E., Guillet, J.E., 1991. Studies of the antenna effect in polymer molecules. 23. Photosensitized dechlorination of 2, 2', 3, 3', 6, 6'-hexachlorobiphenyl solubilized in an aqueous solution of poly (sodium styrenesulfonate-co-2-vinylnaphthalene). *J. Am. Chem. Soc.* 113 (1), 253-258. <https://doi.org/10.1021/ja00001a036>.
- Nowakowska, M., Szczubiałka, K., 2017. Photoactive polymeric and hybrid systems for photocatalytic degradation of water pollutants. *Polym. Degrad. Stab.* 145, 120-141. <https://doi.org/10.1016/j.polymdegradstab.2017.05.021>.
- Organization for Economic Co-operation and Development Report, 2002. ECD; Co-operation on exist chemicals: Hazard Assessment of Perfluorooctane Sulfonate (PFOS) and its Salts (ENV/JM/RD (2002)17/Final). <https://www.oecd.org/env/ehs/risk-assessment/2382880.pdf> (accessed 13 April 2020).
- Olsen, G.W., Church, T.R., Larson, E.B., Van Belle, G., Lundberg, J. K., Hansen, K.J., Burris, J.M., Mandel, J.H., Zobel, L.R., 2004. Serum concentrations of perfluorooctanesulfonate and other fluorochemicals in an elderly population from Seattle, Washington. *Chemosphere* 54, 1599-1611. <https://doi.org/10.1016/j.chemosphere.2003.09.025>.
- O'Neil, M. J. (Ed). 2006. *The Merck Index - An Encyclopedia of Chemicals, Drugs, and Biologicals*. Merck and Co., Inc., New Jersey
- O'Neil, M. J. (ed.). 2013. *The Merck Index - An Encyclopedia of Chemicals, Drugs, and Biologicals*. Royal Society of Chemistry, Cambridge
- Padmanabhan, P.V.A., Sreekumar, K.P., Thiyagarajan, T.K., Satpute, R.U., Bhanumurthy, K., Sengupta, P., Dey, G.K., Warriar, K.G.K., 2006. Nano-crystalline titanium dioxide formed by reactive plasma synthesis. *Vacuum* 80 (11), 1252-1255. <https://doi.org/10.1016/j.vacuum.2006.01.054>.
- Paknikar, K.M., Nagpal, V., Pethkar, A.V., Rajwade, J.M., 2005. Degradation of lindane from aqueous solutions using iron sulfide nanoparticles stabilized by biopolymers. *Sci. Technol. Adv. Mat.* 6 (3-4), 370-374. <https://doi.org/10.1016/j.stam.2005.02.016>.
- Panchangam, S.C., Yellatur, C.S., Yang, J.-S., Loka, S.S., Lin, A.Y. C., Vemula, V., 2018. Facile fabrication of TiO₂-graphene nanocomposites (TGNCs) for the efficient photocatalytic oxidation of perfluorooctanoic acid (PFOA). *J. Environ. Chem. Eng.* 6 (5), 6359-6369. <https://doi.org/10.1016/j.jece.2018.10.003>.

- Pariatamby, A., Kee, Y.L., 2016. Persistent organic pollutants management and remediation. *Procedia Environ. Sci.* 31, 842–848. <https://doi.org/10.1016/j.proenv.2016.02.093>.
- Pascanu, V., González Miera, G., Inge, A.K., Martín-Matute, B., 2019. Metal-Organic frameworks as catalysts for organic synthesis: A critical perspective. *J. Am. Chem. Soc.* 141 (18), 7223–7234. <https://doi.org/10.1021/jacs.9b00733>.
- Pauwels, A., Covaci, A., Weyler, J., Delbeke, L., Dhont, M., De Sutter, P., D'Hooghe, T., Schepens, P.J.C., 2000. Comparison of persistent organic pollutant residues in serum and adipose tissue in a female population in Belgium, 1996–1998. *Arch. Environ. Contam. Toxicol.* 39 (2), 265–270. <https://doi.org/10.1007/s002440010104>.
- Peng, W., Lin, Y., Wan, Z., Ji, H., Ma, W., Zhao, J., 2020. An unusual dependency on the hole-scavengers in photocatalytic reductions mediated by a titanium-based metal-organic framework. *Catal. Today.* 340, 86–91. <https://doi.org/10.1016/j.cattod.2018.11.038>.
- Pham, H.Q., Mai, T., Pham-Tran, N.-N., Kawazoe, Y., Mizuseki, H., Nguyen-Manh, D., 2014. Engineering of band gap in metal-organic frameworks by functionalizing organic linker: a systematic density functional theory investigation. *J. Phys. Chem. C.* 118 (9), 4567–4577. <https://doi.org/10.1021/jp405997r>.
- Pi, Y., Li, X., Xia, Q., Wu, J., Li, Y., Xiao, J., Li, Z., 2018. Adsorptive and photocatalytic removal of Persistent Organic Pollutants (POPs) in water by metal-organic frameworks (MOFs). *Chem. Eng. J.* 337, 351–371. <https://doi.org/10.1016/j.cej.2017.12.092>.
- Rao P. S. C., Davidson J. M. (Eds), 1982. Retention and transformations of selected pesticides and phosphorus in soil-water systems: A critical review. United States Environmental Protection Agency Environmental Research Laboratory, Athens.
- Ren, X., Zeng, G., Tang, L., Wang, J., Wan, J., Liu, Y., Yu, J., Yi, H., Ye, S., Deng, R., 2018. Sorption, transport and biodegradation – An insight into bioavailability of persistent organic pollutants in soil. *Sci. Total Environ.* 610–611, 1154–1163. <https://doi.org/10.1016/j.scitotenv.2017.08.089>.
- Renault, F., Sancey, B., Badot, P.-M., Crini, G., 2009. Chitosan for coagulation/flocculation processes—an eco-friendly approach. *Eur. Polym. J.* 45 (5), 1337–1348. <https://doi.org/10.1016/j.eurpolymj.2008.12.027>.
- Rosberg, M., Lendle, W., Pfeleiderer, G., Tögel, A., Dreher, E. L., Langer, E., Rassaerts, H., Kleinschmidt, P., Strack, H., Cook, R., Beck, U., Lipper, K.-A., Torkelson, T.R., Löser, E., Beutel, K.K., Mann, T., 2006. Chlorinated Hydrocarbons. *Ullmann's Encyclopedia of Industrial Chemistry*, Wiley-VCH, Weinheim. http://dx.doi.org/10.1002/14356007.a06_233.pub2.
- Sakee, U., Wanchanthuek, R., 2017. Catalytic activity of bimetallic Zn/TiO₂ catalyst for degradation of herbicide paraquat: synthesis and characterization. *Mater. Res. Express.* 4, (11). <https://doi.org/10.1088/2053-1591/aa8e59> 115504.
- Saleh, M.A., 1991. Toxaphene: Chemistry, Biochemistry, Toxicity and Environmental Fate. in: Ware, G.W. (Ed) *Reviews of environmental contamination and toxicology*. 118, Springer, New York.
- Samsudin, E.M., Hamid, S.B.A., Juan, J.C., Basirun, W.J., Centi, G., 2015. Enhancement of the intrinsic photocatalytic activity of TiO₂ in the degradation of 1,3,5-triazine herbicides by doping with N. *F. Chem. Eng. J.* 280, 330–343. <https://doi.org/10.1016/j.cej.2015.05.125>.
- Sánchez, B., Coronado, J.M., Candal, R., Portela, R., Tejedor, I., Anderson, M.A., Tompkins, D., Lee, T., 2006. Preparation of TiO₂ coatings on PET monoliths for the photocatalytic elimination of trichloroethylene in the gas phase. *Appl. Catal. B-Environ.* 66 (3), 295–301. <https://doi.org/10.1016/j.apcatb.2006.03.021>.
- Savu, P., 1999. Fluorine-Containing Polymers, Perfluoroalkanesulfonic Acids. *Kirk-Othmer Encyclopedia of Chemical Technology*. John Wiley Sons, New York.
- Schaefer, C., Peters, P., Miller, R. K. (Eds), 2015. *Drugs during pregnancy and lactation: Treatment options and risk assessment*, Academic Press, London. 10.1016/C2011-0-09100-7
- Shaban, Y.A., El Sayed, M.A., El Maradny, A.A., Al Farawati, R. K., Al Zobidi, M.I., Khan, S.U., 2016. Laboratory and pilot-plant scale photocatalytic degradation of polychlorinated biphenyls in seawater using CM-n-TiO₂ nanoparticles. *Int. J. Photoenergy.* 2016. <https://doi.org/10.1155/2016/8471960>.
- Shao, Y.-Y., Ye, W.-D., Sun, C.-Y., Liu, C.-L., Wang, Q., Chen, C.-C., Gu, J.-Y., Chen, X.-Q., 2018. Enhanced photoreduction degradation of polybromodiphenyl ethers with Fe₃O₄-g-C₃N₄ under visible light irradiation. *RSC Adv.* 8 (20), 10914–10921. <https://doi.org/10.1039/c8ra01356j>.
- Shiu, W.Y., Ma, K.C., 2000. Temperature dependence of physical-chemical properties of selected chemicals of environmental interest. II. chlorobenzenes, polychlorinated biphenyls, polychlorinated dibenzo-p-dioxins, and dibenzofurans. *J. Phys. Chem. Ref. Data.* 29, 387–462. <https://doi.org/10.1063/1.1286267>.
- Simpson, C.D., Wilcock, R.J., Smith, T.J., Wilkins, A.L., Langdon, A.G., 1995. Determination of octanol-water partition coefficients for the major components of technical chlordane. *Bull. Environ. Contam. Toxicol.* 55, 149–153. <https://doi.org/10.1007/bf00212402>.
- Song, C., Chen, P., Wang, C., Zhu, L., 2012. Photodegradation of perfluorooctanoic acid by synthesized TiO₂-MWCNT composites under 365 nm UV irradiation. *Chemosphere* 86 (8), 853–859. <https://doi.org/10.1016/j.chemosphere.2011.11.034>.
- Stockholm Convention on Persistent Organic Pollutants
- Su, K., Ai, Z., Zhang, L., 2012. Efficient Visible Light-Driven Photocatalytic Degradation of Pentachlorophenol with Bi₂O₃/TiO_{2-x}B_x. *J. Phys. Chem. C.* 116 (32), 17118–17123. <https://doi.org/10.5004/dwt.2017.21038>.
- Suárez, S., Coronado, J.M., Portela, R., Martín, J.C., Yates, M., Avila, P., Sánchez, B., 2008. On the Preparation of TiO₂-Sepiolite Hybrid Materials for the Photocatalytic Degradation of TCE: Influence of TiO₂ Distribution in the Mineralization. *Environ. Sci. Technol.* 42 (16), 5892–5896. <https://doi.org/10.1021/es703257w>.
- Sun, C., Chen, C., Ma, W., Zhao, J., 2012. Photocatalytic debromination of decabromodiphenyl ether by graphitic carbon nitride. *Sci. China Chem.* 55 (12), 2532–2536. <https://doi.org/10.1007/s11426-012-4644-4>.
- Sustar, E., Nowakowska, M., Guillet, J., 1992. Studies of the antenna effect in polymer molecules 22. Photochemical dechlorination of polychlorinated biphenyls in aqueous solutions of poly (sodium styrenesulfonate-co-2-vinylnaphthalene). *J. Photochem. Photobiol.* 63 (3), 357–365. [https://doi.org/10.1016/1010-6030\(92\)85201-5](https://doi.org/10.1016/1010-6030(92)85201-5).
- Swann, R. L., Laskowski, D. A., McCall, P. J., Vander Kuy, K., Dishburger, H. J., 1983 A rapid method for the estimation of the environmental parameters octanol/water partition coefficient, soil sorption constant, water to air ratio, and water solubility. in: Gunther, F. A., Gunther, J. D. (Eds) *Residue Reviews*. 85, Springer, New York.
- Sweetman, A.J., Dalla Valle, M., Prevedouros, K., Jones, K.C., 2005. The role of soil organic carbon in the global cycling of persistent organic pollutants (POPs): interpreting and modelling field data. *Chemosphere* 60 (7), 959–972. <https://doi.org/10.1016/j.chemosphere.2004.12.074>.
- Szaková, J., Pulkrabová, J., Černý, J., Mercl, F., Švarcová, A., Gramblička, T., Najmanová, J., Tlustoš, P., Balík, J., 2019. Selected persistent organic pollutants (POPs) in the rhizosphere of sewage sludge-treated soil: implications for the biodegradability of POPs. *Arch. Agron. Soil Sci.* 65, 994–1009. <https://doi.org/10.1080/03650340.2018.1543945>.
- Tabak, H.H., Quave, S.A., Mashni, C.I., Barth, E.F., 1981. Biodegradability studies with organic priority pollutant compounds. *J. Water Pollut. Control Fed.* 53 (10), 1503–1518 <https://www.jstor.org/stable/25041532>.
- Tan, T.L., Lai, C.W., Hong, S.L., Rashid, S.A., 2018. New insights into the photocatalytic endocrine disruptors dimethyl phthalate

- esters degradation by UV/MWCNTs-TiO₂ nanocomposites. *J. Photochem. Photobiol.* 364, 177–189. <https://doi.org/10.1016/j.jphotochem.2018.05.019>.
- Tang, Q., Gong, J., Zhao, Q., 2019. Efficient organic pollutant degradation under visible-light using functional polymers of intrinsic microporosity. *Catal. Sci. Technol.* 9 (19), 5383–5393. <https://doi.org/10.1039/c9cy01338e>.
- Tang, C., Huang, X., Wang, H., Shi, H., Zhao, G., 2020. Mechanism investigation on the enhanced photocatalytic oxidation of nonylphenol on hydrophobic TiO₂ nanotubes. *J. Hazard. Mater.* 382. <https://doi.org/10.1016/j.jhazmat.2019.121017>
- Tarkwa, J.B., Oturan, N., Acayanka, E., Laminsi, S., Oturan, M.A., 2019. Photo-Fenton oxidation of Orange G azo dye: process optimization and mineralization mechanism. *Environ. Chem. Lett.* 17, 473–479. <https://doi.org/10.1007/s10311-018-0773-0>.
- ThanhThuy, T.T., Feng, H., Cai, Q., 2013. Photocatalytic degradation of pentachlorophenol on ZnSe/TiO₂ supported by photo-Fenton system. *Chem. Eng. J.* 223, 379–387. <https://doi.org/10.1016/j.cej.2013.03.025>.
- Thomas, J., Chitra, K.R., 2014. Nanogold doped TiO₂ Nanotubes: Efficient solar photocatalyst for the degradation of endosulfan. *Mater. Focus.* 3 (3), 233–238. <https://doi.org/10.1166/mat.2014.1165>.
- Thomas, J., Kumar, K.P., Chitra, K.R., 2011. Synthesis of Ag Doped Nano TiO₂ as Efficient Solar Photocatalyst for the Degradation of Endosulfan. *Adv. Sci. Lett.* 4 (1), 108–114. <https://doi.org/10.1166/asl.2011.1192>.
- Tian, A., Wu, Y., Mao, K., 2017. Enhanced performance of surface modified TiO₂ nanotubes for the decomposition of perfluorooctanoic acid. Paper presented at the AIP Conference Proceedings. <https://doi.org/10.1063/1.4971911>.
- Tian, Y., Zhou, M., Pan, Y., Cai, J., Ren, G., 2020. Pre-magnetized Fe⁰ as heterogeneous electro-Fenton catalyst for the degradation of p-nitrophenol at neutral pH. *Chemosphere* 240. <https://doi.org/10.1016/j.chemosphere.2019.124962>
- Tomlin, C.D.S. (Ed.). 1994. *The Pesticide Manual - World Compendium*. 10th edition., The British Crop Protection Council, Surrey.
- Tran, T.V., Nguyen, D.T.C., Le, H.T.N., Bach, L.G., Vo, D.V.N., Dao, T.U.T., Lim, K.T., Nguyen, T.D., 2019c. Effect of thermolysis condition on characteristics and nonsteroidal anti-inflammatory drugs (NSAIDs) absorbability of Fe-MIL-88B-derived mesoporous carbons. *J. Environ. Chem. Eng.* 7, (5). <https://doi.org/10.1016/j.jece.2019.103356>
- Tran, T.V., Nguyen, D.T.C., Le, H.T., Bach, L.G., Vo, D.V.N., Lim, K.T., Nong, L.X., Nguyen, T.D., 2019d. Combined minimum-run resolution IV and central composite design for optimized removal of the tetracycline drug over metal organic framework templated porous carbon. *Molecules* 24, 1887. <https://doi.org/10.3390/molecules24101887>.
- Tran, T.V., Nguyen, D.T.C., Le, H.T.N., Bach, L.G., Vo, D.V.N., Hong, S.S., Phan, T.Q.T., Nguyen, T.D., 2019e. Tunable synthesis of mesoporous carbons from Fe₃O(Bdc)₃ for chloramphenicol antibiotic remediation. *Nanomaterials.* 9 (2), 237. <https://doi.org/10.3390/nano9020237>.
- Tran, T.V., Cam Nguyen, D.T., Le, H.T., Nguyen, O.T., Nguyen, V. H., Nguyen, T.T., Bach, L.G., Nguyen, T.D., 2019a. A hollow mesoporous carbon from metal-organic framework for robust adsorbability of ibuprofen drug in water. *R. Soc. Open Sci.* 6, (5). <https://doi.org/10.1098/rsos.190058>.
- Tran, T.V., Nguyen, D.T.C., Nguyen, H.T.T., Nanda, S., Vo, D.V. N., Do, S.T., Van Nguyen, T., Thi, T.A.D., Bach, L.G., Nguyen, T. D., 2019b. Application of Fe-based metal-organic framework and its pyrolysis products for sulfonamide treatment. *Environ. Sci. Pollut. Res.* 26, 28106–28126. <https://doi.org/10.1007/s11356-019-06011-2>.
- Tran, T.V., Dai Cao, V., Nguyen, V.H., Hoang, B.N., Vo, D.V.N., Nguyen, T.D., Bach, L.G., 2020. MIL-53 (Fe) derived magnetic porous carbon as a robust adsorbent for the removal of phenolic compounds under the optimized conditions. *J. Environ. Chem. Eng.* 8, (1). <https://doi.org/10.1016/j.jece.2019.102902>
- U.S. Environmental Protection Agency Report, 1977. *The Degradation of Selected Pesticides in Soil: A Review of Published Literature USEPA-600/9-77-022*. https://cfpub.epa.gov/si/si_public_record_Report.cfm?Lab=ORD&dirEntryID=30082 (accessed 18 April 2020).
- Umebayashi, T., Yamaki, T., Itoh, H., Asai, K., 2002. Band gap narrowing of titanium dioxide by sulfur doping. *Appl. Phys. Lett.* 81 (3), 454–456. <https://doi.org/10.1063/1.1493647>.
- Persistent Organic Pollutants Review Committee Third meeting, 2007. *Commercial Pentabromodiphenyl Ether: Risk Management Evaluation*. <http://chm.pops.int/Portals/0/download.aspx?d=UNEP-POPS-POPRC.3-20-Add.1.English.PDF> (accesses 18 April 2020).
- United States Environmental Protection Agency's Integrated Risk Information System (IRIS). Summary on beta-Hexachlorocyclohexane (beta-HCH) (319-85-7), 2020. Available from, as of: <http://www.epa.gov/iris/> (accessed 13 April 2020)
- United States Environmental Protection Agency Status of Pesticides in Registration, Reregistration, and Special Review USEPA 738-R-98-002, 1998 Washington, DC., pp. 44
- Vaalgamaa, S., Vähätalo, A.V., Perkola, N., Huhtala, S., 2011. Photochemical reactivity of perfluorooctanoic acid (PFOA) in conditions representing surface water. *Sci. Total Environ.* 409 (16), 3043–3048. <https://doi.org/10.1016/j.scitotenv.2011.04.036>.
- Velasco, L.F., Parra, J.B., Ania, C.O., 2010. Role of activated carbon features on the photocatalytic degradation of phenol. *Appl. Surf. Sci.* 256 (17), 5254–5258. <https://doi.org/10.1016/j.apsusc.2009.12.113>.
- Vergura, E.P., Garcia-Ballestreros, S., Vercher, R.F., Santos-Juanes, L., Prevot, A.B., Arques, A., 2019. Photo-Fenton degradation of pentachlorophenol I: competition between additives and photolysis. *Nanomaterials.* 9 (8), 1157. <https://doi.org/10.3390/nano9081157>.
- Verma, A.K., Dash, R.R., Bhunia, P., 2012. A review on chemical coagulation/flocculation technologies for removal of colour from textile wastewaters. *J. Environ. Manage.* 93 (1), 154–168. <https://doi.org/10.1016/j.jenvman.2011.09.012>.
- Vlotman, D.E., Ngila, J.C., Ndlovu, T., Doyle, B., Carleschi, E., Malinga, S.P., 2019. Hyperbranched polymer membrane for catalytic degradation of polychlorinated biphenyl-153 (PCB-153) in water. *React. Funct. Polym.* 136, 44–57. <https://doi.org/10.1016/j.reactfunctpolym.2018.12.019>.
- Wang, Q., Gao, Q., Al-Enizi, A. M., Nafady, A., Ma, S., 2020. Recent advances in MOF-based photocatalysis: environmental remediation under visible light. *Inorg. Chem. Frontiers.* 10.1039/c9qi01120j.
- Wang, R., Tang, T., Wei, Y., Dang, D., Huang, K., Chen, X., Yin, H., Tao, X., Lin, Z., Dang, Z., Lu, G., 2019. Photocatalytic debromination of polybrominated diphenyl ethers (PBDEs) on metal doped TiO₂ nanocomposites: Mechanisms and pathways. *Environ. Int.* 127, 5–12. <https://doi.org/10.1016/j.envint.2019.03.011>.
- Wang, H., Wang, H.-L., Jiang, W.-F., 2009. Solar photocatalytic degradation of 2,6-dinitro-p-cresol (DNPC) using multi-walled carbon nanotubes (MWCNTs)-TiO₂ composite photocatalysts. *Chemosphere* 75 (8), 1105–1111. <https://doi.org/10.1016/j.chemosphere.2009.01.014>.
- Wang, S., Wang, J., 2018. Trimethoprim degradation by Fenton and Fe(II)-activated persulfate processes. *Chemosphere* 191, 97–105. <https://doi.org/10.1016/j.chemosphere.2017.10.040>.
- Wang, J., Yang, H., Jiang, L., Liu, S., Hao, Z., Cheng, J., Ouyang, G., 2018. Highly efficient removal of organic pollutants by ultrahigh-surface-area-ethynylbenzene-based conjugated microporous polymers via adsorption-photocatalysis synergy. *Catal. Sci. Technol.* 8 (19), 5024–5033. <https://doi.org/10.1039/c8cy01379a>.
- Wang, Y., Zhang, P., 2011. Photocatalytic decomposition of perfluorooctanoic acid (PFOA) by TiO₂ in the presence of oxalic acid. *J.*

- Hazard. Mater. 192 (3), 1869–1875. <https://doi.org/10.1016/j.jhazmat.2011.07.026>.
- Wang, B., Zhang, C., Li, Shuying, Lu, Guangqiu, Lu, Guoli, Li, Song, Zhou, Y., 2016. An approach to biodegradation of chlorobenzenes: Combination of *Typha angustifolia* and bacterial effects on hexachlorobenzene degradation in water. Water Sci. Technol. 74 (6), 1409–1416. <https://doi.org/10.2166/wst.2016.313>.
- Wantala, K., Khamjumhol, C., Thananukool, N., Neramittagapong, A., 2015. Degradation of Reactive Red 3 by heterogeneous Fenton-like process over iron-containing RH-MCM-41 assisted by UV irradiation. Desalin. Water Treat. 54, 699–706. <https://doi.org/10.1080/19443994.2014.886295>.
- Wantala, K., Chansiriwata, W., Khunphonib, R., Kaewbuddeea, C., Suwannaruanga, T., Chanlekf, N., Grisdanurakg, N., 2019. Optimization and mechanism pathways of p-cresol decomposition over Cu-Fe/NaPI catalyst by Fenton-like process. Desalin. Water Treat. 166, 122–134. <https://doi.org/10.5004/dwt.2019.24633>.
- World Health Organization, 1994. Environmental Health Criteria 162. Brominated Diphenyl Ethers, Geneva.
- Wu, C.H., Chang-Chien, G.P., Lee, W.S., 2004. Photodegradation of polychlorinated dibenzo-p-dioxins: comparison of photocatalysis. J. Hazard. Mater. B114, 191–197. <https://doi.org/10.1016/j.jhazmat.2004.08.008>.
- Wu, C.H., Chang-Chien, G.P., Lee, W.S., 2005. Photodegradation of tetra- and hexachlorodibenzo-p-dioxins. J. Hazard. Mater. 120 (1–3), 257–263. <https://doi.org/10.1016/j.jhazmat.2005.01.014>.
- Wu, C.H., Ng, H.Y., 2008. Photodegradation of polychlorinated dibenzo-p-dioxins and polychlorinated dibenzofurans: direct photolysis and photocatalysis processes. J. Hazard. Mater. 151, 507–514. <https://doi.org/10.1016/j.jhazmat.2007.06.020>.
- Wyrzykowska-Ceradini, B., Gullett, B.K., Tabor, D., Touati, A., 2011. Waste combustion as a source of ambient air polybrominated diphenylethers (PBDEs). Atmos. Environ. 45, 4008–4014. <https://doi.org/10.1016/j.atmosenv.2011.04.052>.
- Xia, Q., Li, Z., Xi, H., Xu, K., 2005. Activation Energy for Dibenzofuran Desorption from Fe³⁺/TiO₂ and Ce³⁺/TiO₂ Photocatalysts Coated onto Glass Fibres. Adsorp. Sci. Technol. 23 (5), 357–366. <https://doi.org/10.1260/026361705774355469>.
- Xia, S., Shao, M., Zhou, X., Pan, G., Ni, Z., 2015. Ti/ZnO–MxOy composites (M = Al, Cr, Fe, Ce): synthesis, characterization and application as highly efficient photocatalysts for hexachlorobenzene degradation. Phys. Chem. Chem. Phys. 17 (40), 26690–26702. <https://doi.org/10.1039/C5CP04125B>.
- Xiao, Z., Huang, X., Zhao, K., Song, Q., Guo, R., Zhang, X., Zhou, S., Kong, D., Wagner, M., Müllen, K., Zhi, L., 2019. Band Structure Engineering of Schiff-Base Microporous Organic Polymers for Enhanced Visible-Light Photocatalytic Performance. Small. 15 (34), 1900244. <https://doi.org/10.1002/sml.201900244>.
- Xu, J., Shimakoshi, H., Hisaeda, Y., 2015. Development of metal-organic framework (MOF)-B12 system as new bio-inspired heterogeneous catalyst. J. Organomet. Chem. 782, 89–95. <https://doi.org/10.1016/j.jorganchem.2014.11.015>.
- Xu, W., Wang, X., Cai, Z., 2013. Analytical chemistry of the persistent organic pollutants identified in the Stockholm Convention: A review. Anal. Chim. Acta. 790, 1–13. <https://doi.org/10.1016/j.aca.2013.04.026>.
- Yadav, S.K., 2010. Pesticide Applications-Threat to Ecosystems. J. Hum. Ecol. 32 (1), 37–45. <https://doi.org/10.1080/09709274.2010.11906319>.
- Yang, J., Zhang, Y., Zeng, D., Zhang, B., Hassan, M., Li, P., Qi, C., He, Y., 2020. Enhanced catalytic activation of photo-Fenton process by Cu_{0.5}Mn_{0.5}Fe₂O₄ for effective removal of organic contaminants. Chemosphere 247, <https://doi.org/10.1016/j.chemosphere.2019.125780> 125780.
- Yao, Y., Li, G., Ciston, S., Lueptow, R.M., Gray, K.A., 2008. Photoreactive TiO₂/Carbon Nanotube Composites: Synthesis and Reactivity. Environ. Sci. Technol. 42 (13), 4952–4957. <https://doi.org/10.1021/es800191n>.
- Yin, H., Wada, Y., Kitamura, T., Yanagida, S., 2001. Photoreductive dehalogenation of halogenated benzene derivatives using ZnS or CdS nanocrystallites as photocatalysts. Environ. Sci. Technol. 35 (1), 227–231. <https://doi.org/10.1021/es001114d>.
- Yola, M.L., Eren, T., Atar, N., 2014. A novel efficient photocatalyst based on TiO₂ nanoparticles involved boron enrichment waste for photocatalytic degradation of atrazine. Chem. Eng. J. 250, 288–294. <https://doi.org/10.1016/j.cej.2014.03.116>.
- Youssef, L., El-Rassy, H., Younes, G., Al-Oweini, R., 2019. Photocatalytic and Kinetic Study on the Degradation of Three Food Pesticides Using Vanadium-Substituted Polyoxotungstates. Int. J. Environ. Res. 13 (6), 899–907. <https://doi.org/10.1007/s41742-019-00226-4>.
- Yu, L., Yang, X., Ye, Y., Peng, X., Wang, D., 2015. Silver nanoparticles decorated anatase TiO₂ nanotubes for removal of pentachlorophenol from water. J. Colloid Interface Sci. 453, 100–106. <https://doi.org/10.1016/j.jcis.2015.04.057>.
- Yu, B., Zeng, J., Gong, L., Zhang, M., Zhang, L., Chen, X., 2007. Investigation of the photocatalytic degradation of organochlorine pesticides on a nano-TiO₂ coated film. Talanta 72 (5), 1667–1674. <https://doi.org/10.1016/j.talanta.2007.03.013>.
- Zakaria, Z., Heng, L.Y., Abdullah, P., Osman, R., Din, L., 2003. The environmental contamination by organochlorine insecticides of some agricultural areas in Malaysia. Mal J Chem. 5, 078–085.
- Zaleska, A., Hupka, J., Wierowski, M., Biziuk, M., 2000. Photocatalytic degradation of lindane, p, p'-DDT and methoxychlor in an aqueous environment. J. Photochem. Photobiol. A. 135 (2–3), 213–220. [https://doi.org/10.1016/S1010-6030\(00\)00296-3](https://doi.org/10.1016/S1010-6030(00)00296-3).
- Zhang, H., Liang, C., Liu, J., Tian, Z., Wang, G., Cai, W., 2012. Defect-Mediated Formation of Ag Cluster-Doped TiO₂ Nanoparticles for Efficient Photodegradation of Pentachlorophenol. Langmuir 28 (8), 3938–3944. <https://doi.org/10.1021/la2043526>.
- Zhang, M., Lu, J., He, Y., Wilson, P.C., 2016. Photocatalytic degradation of polybrominated diphenyl ethers in pure water system. Front. Environ. Sci. Eng. 10 (2), 229–235. <https://doi.org/10.1007/s11783-014-0762-x>.
- Zhang, X., Tang, Y., Li, Y., Wang, Y., Liu, X., Liu, C., Luo, S., 2013. Reduced graphene oxide and PbS nanoparticles co-modified TiO₂ nanotube arrays as a recyclable and stable photocatalyst for efficient degradation of pentachlorophenol. Appl. Catal. A. 457, 78–84. <https://doi.org/10.1016/j.apcata.2013.03.011>.
- Zhao, X., Quan, X., Zhao, H., Chen, S., Zhao, Y., Chen, J., 2004. Different effects of humic substances on photodegradation of p, p'-DDT on soil surfaces in the presence of TiO₂ under UV and visible light. J. Photochem. Photobiol. 167 (2), 177–183. <https://doi.org/10.1016/j.jphotochem.2004.05.003>.
- Zhao, H., Zhang, F., Qu, B., Xue, X., Liang, X., 2009. Wet air co-oxidation of decabromodiphenyl ether (BDE209) and tetrahydrofuran. J. Hazard. Mater. 169 (1–3), 1146–1149. <https://doi.org/10.1016/j.jhazmat.2009.03.089>.
- Zhu, C., Fang, G., Dionysiou, D.D., Liu, C., Gao, J., Qin, W., Zhou, D., 2016. Efficient transformation of DDTs with persulfate activation by Zero-valent iron nanoparticles: A mechanistic study. J. Hazard. Mater. 316, 232–241. <https://doi.org/10.1016/j.jhazmat.2016.05.040>.
- Zoeteman, B.C.J., Harmsen, K., Linders, J.B.H.J., Morra, C.F.H., Slooff, W., 1980. Persistent organic pollutants in river water and ground water of the Netherlands. Chemosphere 9, 231–249. [https://doi.org/10.1016/0045-6535\(80\)90080-6](https://doi.org/10.1016/0045-6535(80)90080-6).
- Zubair, M., Adrees, A., 2019. Dioxins and Furans: Emerging Contaminants of Air, in: Air Pollution - Monitoring, quantification and removal of gases and particles, Olvera, J. D. R. (Ed). Intech Open, London. 10.5772/intechopen.80680.